Received: 29 April 2020 | Revised: 2 March 2021 | Accepted: 3 March 2021

DOI: 10.1002/rnc.5500

RESEARCH ARTICLE

WILEY

Quantized control for a class of neural networks with adaptive event-triggered scheme and complex cyber-attacks

Jinliang Liu[1,2] | Wei Suo[1] | Xiangpeng Xie[3] | Dong Yue[3] | Jinde Cao[4]

[1]College of Information Engineering, Nanjing University of Finance and Economics, Nanjing, China

[2]Key Laboratory of Information Perception and Cooperative Control of Multi-mobiles, Nanjing, China

[3]Institute of Advanced Technology, Nanjing University of Posts and Telecommunications, Nanjing, China

[4]School of Mathematics, and Research Center for Complex Systems and Network Sciences, Southeast University, Nanjing, China

Correspondence
Jinliang Liu, College of Information Engineering, Nanjing University of Finance and Economics, Nanjing 210023, China.
Email: liujinliang@vip.163.com

Funding information
National Natural Science Foundation of China, Grant/Award Number: 61973152

Abstract

This article is concerned with the quantized control problem for neural networks with adaptive event-triggered scheme (AETS) and complex cyber-attacks. By fully considering the characteristics of cyber-attacks, a mathematical model of complex cyber-attacks, which consists of replay attacks, deception attacks, and denial-of-service (DoS) attacks, is firstly built for neural networks. For the sake of relieving the pressure under limited communication resources, an AETS and a quantization mechanism are employed in this article. By utilizing Lyapunov stability theory, adequate conditions ensuring the stability of neural networks are obtained. Moreover, the controller gain is derived by solving a set of linear matrix inequalities. At last, the usefulness of the proposed method is verified by a numerical example.

KEYWORDS

adaptive event-triggered scheme (AETS), complex cyber-attacks, neural networks, quantization mechanism

1 | INTRODUCTION

Due to the satisfactory nonlinear approximation and learning abilities, neural networks have been extensively applied in modeling of nonlinear networked systems[1-5] to solve the synthetic control problems, such as the robust stability,[6] controller design,[7] and so on. For example, the authors of Reference 8 studied the exponential stability analysis problem for generalized neural networks with time delays. In Reference 9, the robust stabilization problem was addressed for continuous-time delayed neural networks via dissipativity-learning approach. The authors of Reference 10 investigated H_∞ filtering problem for stochastic neural networks with a mixed of time-varying interval delays, time-varying distributed delays, and leakage delays. The authors of Reference 11 concentrated on solving the adaptive neural network control issue for bilateral teleoperation system with dynamic uncertainties.

With the rapid development of network communication technologies, the network plays a more and more important role in the networked systems. Since the network resources is limited, how to deal with network resource constraints are a fundamental research topic for studying networked systems. In the past few years, the time-triggered schemes and the event-triggered schemes (ETSs) are two widely used data transmission strategies. Under the time-triggered schemes, the signals are periodically delivered in a fixed time period. Nevertheless, when there is little fluctuation of the delivered data, transmitting the almost identical data through communication network may cause the waste of communication resources. To deal with the above problem, numerous scholars have proposed multifarious ETS.[12-18]

Specially, the adaptive ETS (AETS) has an advantage over traditional ETSs in relieving the network bandwidth load owing to the adjusted threshold, thus it has captured great attention.[19-22] For instance, the authors of Reference 23 applied AETS to economize limited transmission resources for uncertain active suspension systems. H_∞ filtering problem was addressed for a class of networked nonlinear interconnected systems with AETS in Reference 24. In addition to ETS, quantization is considered as another effective tool to save the limited bandwidth. By using quantization mechanism, the continuous signal are converted into a set of discrete signal to reduce redundant data. The applications of quantization mechanism for various systems can be found in considerable literature.[25-29] For instance, the authors of Reference 30 investigated the feedback control issue for networked systems with quantization. In Reference 31, H_∞ filtering problem was addressed for switched systems with quantization. The consensus control problem was studied for multi-agent systems with quantization in Reference 32. By applying quantization mechanism to uncertain linear systems, the authors of Reference 33 investigated the fault tolerant compensation control issue.

Owing to the insertion of network, it brings many advantages to networked systems, such as timeliness, convenience and high efficiency. Nevertheless, due to the openness of networked communication channels, networked systems are vulnerable to malicious cyber-attacks. In view of this, great efforts has been made to deal with the cyber security problems for networked systems. Some control and estimation problems for networked systems have been carefully studied with common attacks including replay attacks,[34] deception attacks,[35] and denial-of-service (DoS) attacks,[36,37] and so on. When replay attacks occur, the attackers record a series of sampled data and replay the ones afterwards. Different from the replay attacks, attackers launch deception attacks by replacing the normal data with malicious data. Stabilization control problem was studied for networked systems subjected to deception attacks in Reference 35. As another common attacks, DoS attacks try to jam the data transmission channels to prevent the measurement and sampled data from reaching their destinations. Taking the impact of DoS attacks into account, the problem of robust stabilization was studied for uncertain networked control systems in Reference 36. However, most of the existing achievements are only concerned with one kind of cyber-attacks, which is not realistic. In fact, the systems may suffer from various cyber-attacks at the same time. In order to reflect the actual situation, three common cyber-attacks are considered including replay attacks, deception attacks, and DoS attacks in this article. To the best of our knowledge, there are no relevant results about the quantized control for neural networks with AETS and complex cyber-attacks, which motivates this current work.

In this article, by applying an AETS, the problem of quantized control for neural networks under complex cyber-attacks will be investigated. An AETS is adopted to save the limited communication resources. A quantization mechanism is introduced to further save the limited resources. Complex cyber-attacks will be taken into consideration which consist of replay attacks, deception attacks and DoS attacks.

The remaining part of this article is organized as follows. Section 2 presents the model of quantized control for neural networks with AETS and complex cyber-attacks. Sufficient conditions, which ensure the stability of neural networks, are obtained in Section 3. Besides, the desired controller gain is acquired. In Section 4, a simulation example is given to verify the effectiveness of the designed controller. At last, a conclusion is given in Section 5.

Notation: $\mathbb{R}^n$ denotes the n-demonsional Euclidean space; $\mathbb{R}^{n\times m}$ denotes the set of $n \times m$ real matrices. $\|\cdot\|$ represents the Euclidean vector norm or the induced matrix 2-norm as appropriate. The superscript T denotes the matrix transposition. I is the identity matrix with appropriate dimension. $sym\{X\}$ represents the sum of matrix X and its transposed matrix X^T.

2 | PROBLEM FORMULATION

2.1 | System description

Consider the following n-neuron delayed neural network

$$\begin{cases} \dot{x}(t) = Ax(t) + Bu(t) + Eg(x(t-\eta(t))) \\ z(t) = Cx(t) \end{cases} \tag{1}$$

where $x(t) = [x_1(t) \quad \dots \quad x_n(t)]^T \in \mathbb{R}^n$ is the state vector of neural networks; $u(t) \in \mathbb{R}^n$ denotes the control input; $z(t) \in \mathbb{R}^n$ represents the measurement output; $g(x(t)) = \left[g_1(x_1(t)) \quad \dots \quad g_n(x_n(t))\right]^T$ represents the neuron activation function

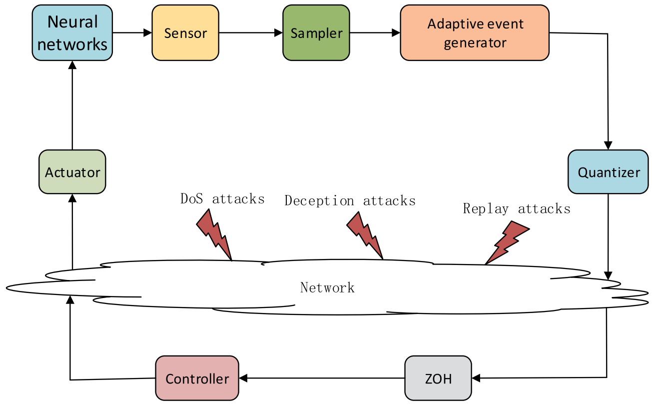

FIGURE 1 The structure of quantized control for neural networks with AETS and complex cyber-attacks [Colour figure can be viewed at wileyonlinelibrary.com]

with $g(0) = 0$; $\eta(t)$ denotes the time delay which satisfies the thresholds $0 \leq \eta(t) \leq \eta_M$, and η_M is a constant; the diagonal matrix $A = diag\{a_1, a_2, \dots, a_n\} < 0$; B, C, and E are given matrices with appropriate dimensions.

Assumption 1 (9). The activation function $g(x(t))$ satisfies the following condition with bounded property:

$$\gamma_g^- \leq \frac{g(\xi_1) - g(\xi_2)}{\xi_1 - \xi_2} \leq \gamma_g^+$$

where γ_g^- and γ_g^+ are known constants, for all $\xi_1, \xi_2 \in \mathbb{R}$, $\xi_1 \neq \xi_2$.

The main purpose of this article is to design a quantized controller for neural networks with AETS and complex cyber-attacks. The structure of feedback control for neural networks is shown in Figure 1. A quantization mechanism and an AETS are employed to mitigate the network bandwidth load. A zero-order-holder (ZOH) is introduced between the network and the controller. The quantized data is delivered to the controller via network subjected to complex cyber-attacks.

In this article, the designed controller is given as follows

$$u(t) = Kx(t) \tag{2}$$

where $K \in \mathbb{R}^{n \times m}$ denotes the controller gain to be designed.

2.2 | Adaptive event-triggered scheme

As shown in Figure 1, an AETS is adopted to relieve the network bandwidth load in this article. Let $\{t_0h, t_1h, t_2h, \dots\}$ represent the transmitted instants. The instant t_0h represents the first triggering time. t_kh is the latest transmission instant, then the next transmission instant $t_{k+1}h$ can be expressed as follows:

$$t_{k+1}h = t_kh + min\{qh|e_k^T(t_kh)\Omega e_k(t_kh) > \pi(t)x^T(t_kh + qh)\Omega x(t_kh + qh)\} \tag{3}$$

where $\Omega > 0$, $e_k(t_kh) = x(t_kh) - x(t_kh + qh)$, $e_k(t_kh)$ denotes the error state between the latest data and current sampling data; $x(t_kh)$ denotes the latest transmitted data, $x(t_kh + qh)$ denotes the current sampling data, $\pi(t)$ is a function satisfying the following adaptive law

$$\dot{\pi}(t) = \frac{1}{\pi(t)} \left(\frac{1}{\pi(t)} - \sigma \right) e_k^T(t)\Omega e_k(t) \tag{4}$$

where $0 < \pi(0) \leq 1$, $\sigma > 0$.

Remark 1. From (3), one can get that the threshold of AETS is a varying parameter, which is regulated by the adaptive law in (4). The AETS, in which the triggering condition can be dynamically adjusted depending on the error state, shows flexibility in transmitting the sampled data. Inspired by [38], an AETS is applied to controller design for neural networks in this article.

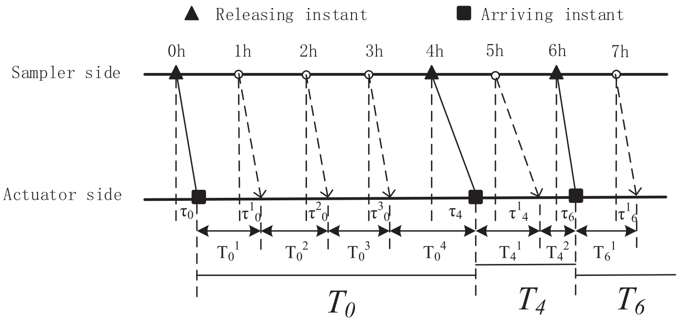

FIGURE 2 An example of time sequence for an AETS

Remark 2. In (4), when the parameter $\sigma = \frac{1}{\pi(0)}$, one can get the adaptive event-triggered law $\dot{\pi}(t) \equiv 0$. It means that the proposed AETS reduces to general time-triggered scheme. If the system gradually reaches stable, the adaptive law $\dot{\pi}(t) \rightarrow 0$, it denotes that the threshold of AETS does not need to be regulated.

The interval $[t_k h + \tau_k, t_{k+1} h + \tau_{t_{k+1}})$ can be divided into several parts as $T_{t_k}^q = [t_k h + qh - h + \tau_{t_k}^{q-1}, t_k h + qh + \tau_{t_k}^q)$ for $q = 1, 2, \ldots, \hat{q}$, where $\hat{q}$ represents the number of subintervals. $\tau_{t_k}^q$ is a positive constant. $\tau_{t_k}^q$ takes the value of τ_{t_k} and $\tau_{t_{k+1}}$ for $q \leq \hat{q} - 1$ and $q = \hat{q}$, respectively. In brief, $T_{t_k} = \cup_{q=1}^{\hat{q}} T_{t_k}^q$. As shown in Figure 2, ▲ denotes the releasing instant, ■ represents the arriving instant, and h is sampling period. The data are sampled periodically at instants $0h, 1h, \ldots$,. In particular, the data are discarded at instants $1h, 2h, 3h, 5h, 7h, \ldots$ on account of not reaching the triggering condition. The data at instants $0h, 4h, 6h, \ldots$ satisfying the condition are delivered by network. τ_0^1 is a transmitted delay of sampled data at instant $1h$; the releasing interval T_0 contains a set of sampling-like subsets T_0^1, T_0^2, T_0^3, T_0^4.

Set $\Sigma \triangleq \{q | e_k^T(t)\Omega e_k(t) - \pi(t) x^T(t_k h + qh)\Omega x(t_k h + qh) \leq 0\}$, then $\hat{q}$ can be defined by

$$\hat{q} = \begin{cases} 1, & \Sigma = \emptyset \\ 1 + max\{q | q \in \Sigma\}, & others \end{cases} \tag{5}$$

The triggering condition of AETS can be expressed as follows

$$e_k^T(t)\Omega e_k(t) - \pi(t) x^T(t_k h + qh)\Omega x(t_k h + qh) < 0 \tag{6}$$

Define the equivalent delay $\tau(t) = t - (t_k h + qh)$, then the sampled data via AETS can be acquired as follows:

$$\hat{x}(t) = x(t - \tau(t)) + e_k(t) \tag{7}$$

where $\tau(t)$ is time-varying delay satisfying $0 \leq \tau(t) \leq \tau_M$, τ_M is a positive constant.

Assumption 2. In this article, we assume that the actuator is event-triggered, while the sensor is time-triggered. A ZOH is adopted to keep the current control input in case that the latest input is not transmitted to the controller. The data in communication network is delivered with a single packet.

2.3 | Quantization mechanism

In order to further save the limited bandwidth, a logarithmic quantizer shown in Figure 3 is employed to decrease the redundant data with linear quantization levels. Suppose that the set of quantization levels is described by $H = \{\pm l_v : l_v = \vartheta_v l_0, v = \pm 1, \pm 2, \ldots\} \cup \{\pm l_0\} \cup \{0\}, l_0 > 0$.

The logarithmic quantizer can be defined as follows:

$$r(x_v) = \begin{cases} l_v, x_v > 0, \frac{l_v}{1+b} < x_v < \frac{l_v}{1-b} \\ 0, x_v = 0 \\ -r(-x_v), x_v < 0 \end{cases} \tag{8}$$

FIGURE 3 The logarithmic quantizer

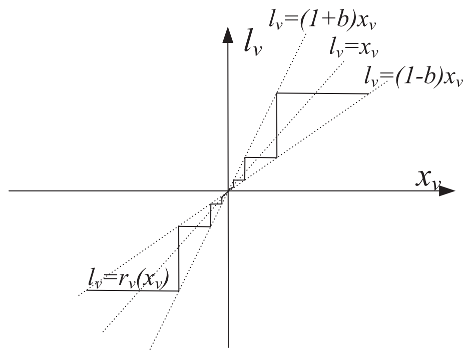

where $b = \frac{1-\vartheta}{1+\vartheta}$; $0 < \vartheta < 1$; ϑ is regarded as quantization density of $r(\cdot)$. If $x = [x_1, x_2, \dots, x_m]^T \in \mathbb{R}^m$ is an m-dimensional vector signal, then one can denote $r(x) = \text{diag}\{r_1(x_1), r_2(x_2), \dots, r_m(x_m)\}$. For the symmetrical matrix $r_v(\cdot), v \in \mathbb{R}^m$, the equality $r_v(-x_v) = -r_v(x_v)$ holds. The logarithmic quantizer $r_v(\cdot)$ can be expressed as

$$r_v(x_v) = (I + \Delta_{r_v}(x_v))x_v \tag{9}$$

where $|\Delta_{r_v}(x_v))| \leq b_v$. For simplicity, Δ_r is utilized to represent $\Delta_{r_v}(x_v))$. One can get the following equality

$$r(x) = (I + \Delta_r)x \tag{10}$$

where $\Delta_r = diag\{\Delta_{r_1}, \Delta_{r_2}, \dots, \Delta_{r_m}\}$.

By combining equalities (7) and (10), the delivered data through the quantizer can be obtained

$$\tilde{x}(t) = (I + \Delta_r)\hat{x}(t) \tag{11}$$

Remark 3. There exist two types of common quantizers including static quantizers and dynamic quantizers. As one of the most representative static quantizers, the logarithmic quantizer is widely used in overcoming the constraint of the network bandwidth. Compared with the dynamic quantizer, the logarithmic quantizer is more efficient due to its simpler implementation. Therefore, a logarithmic quantizer is introduced to save the limited bandwidth in this article.

2.4 | Complex cyber-attacks model

In this subsection, a complex cyber-attacks model, where replay attacks, deception attacks and DoS attacks are taken into account, will be constructed for neural networks. In the following, the replay attacks, deception attacks and DoS attacks are discussed in turn as shown in Figure 1.

First, replay attacks are considered, in which attackers can record a series of sensor data and replay the sequence afterwards. A random variable $\varepsilon(t)$ obeying Bernoulli distribution is utilized to describe whether the replay attacks occur or not. The delivered signal under replay attacks can be acquired

$$\tilde{x}_1(t) = \varepsilon(t)x_r(t) + (1 - \varepsilon(t))\tilde{x}(t) \tag{12}$$

where $x_r(t) = \tilde{x}(t_r)$, $\tilde{x}(t_r)$ represents the transmitted data at the past-time moment. For $\varepsilon(t) \in \{0, 1\}$, the expectation of $\varepsilon(t)$ can be expressed as $\mathbb{E}\{\varepsilon(t)\} = \bar{\varepsilon}$; the mathematical variance of $\varepsilon(t)$ can be expressed as $\mathbb{E}\{(\varepsilon(t) - \bar{\varepsilon})^2\} = \delta_1^2$. $\varepsilon(t) = 0$ represents that the replay attacks are not occurring; $\varepsilon(t) = 1$ denotes that the network suffers from replay attacks.

In addition, deception attacks are considered, which aim to replace legally sampled data with malicious data. With the same method in modeling replay attacks, a Bernoulli variable $\varrho(t)$ is adopted to describe whether deception attacks occur or not. The following equality denotes the transmitted data with deception attacks.

$$\tilde{x}_2(t) = \varrho(t)f(x(t - d(t))) + (1 - \varrho(t))\tilde{x}_1(t) \tag{13}$$

where $f(x(t)) = \begin{bmatrix} f_1(x_1(t)) & \dots & f_n(x_n(t)) \end{bmatrix}^T \in \mathbb{R}^n$ denotes the function of deception attacks. $d(t)$ is time-varying delay satisfying $0 \leq d(t) \leq d_M$, where d_M is a positive constant. The Bernoulli variable $\varrho(t) \in \{0, 1\}$ is with given statistical properties: expectation $\mathbb{E}\{\varrho(t)\} = \overline{\varrho}$ and variance $\mathbb{E}\{\varrho(t) - \overline{\varrho}\} = \delta_2^2$. $\varrho(t) = 0$ means that the deception attacks fail to change the normal transmission data. $\varrho(t) = 1$ denotes that deception attacks have replaced normal data with false data.

Remark 4. When $\varepsilon(t) = 0$ and $\varrho(t) = 0$, replay attacks and deception attacks are not occurring; when $\varepsilon(t) = 1$ and $\varrho(t) = 0$, only the replay attacks are active; when $\varepsilon(t) = 0$ and $\varrho(t) = 1$ represent the network only suffers from deception attacks.

Assumption 3. In this article, we consider that the transmitted data may be subject to deception attacks and replay attacks randomly. We assume that the Bernoulli distributed variable $\varepsilon(t) \in \{0, 1\}$ is used to describe the randomness of the replay attacks, and the Bernoulli variable $\varrho(t) \in \{0, 1\}$ is adopted to describe whether deception attacks occur or not.

Assumption 4. For a constant matrix G, the deception attacks signal $f(x(t))$ satisfies the following constraint.

$$\|f(x(t))\|_2 \leq \|Gx(t)\|_2 \tag{14}$$

where G is a given matrix with appropriate dimension representing the upper bound of deception attacks.

At last, nonperiodic DoS attacks are considered which attempt to prevent the normal data transmission by occupying communication resources. In general, the DoS attacks are irregular and random. The nonperiodic DoS attacks signal with variable $v(t)$ can be expressed as follows

$$v(t) = \begin{cases} 0, t \in [w_n, w_n + \epsilon_n) \\ 1, t \in [w_n + \epsilon_n, w_{n+1}) \end{cases} \tag{15}$$

where $v(t) = 0$ means that the systems are under safe condition and the data transmission is normal; $v(t) = 1$ denotes that DoS attacks are active. $n \in \mathbb{N}$, w_n denotes the starting instant of n_{th} DoS sleeping intervals. $w_n + \epsilon_n$ represents the ending instant of n_{th} DoS sleeping intervals; $w_{n+1} - w_n - \epsilon_n$ denotes the length of $(n+1)_{th}$ DoS active intervals. The DoS attacks intervals can be expressed as $\mathcal{M}_n = [w_n, w_n + \epsilon_n)$ and $\mathcal{N}_n = [w_n + \epsilon_n, w_{n+1})$. w_{n+1} and $w_n + \epsilon_n$ should satisfy the condition $w_{n+1} > w_n + \epsilon_n$.

By considering the impact of complex cyber-attacks, the real control input is given

$$\tilde{x}_3(t) = (1 - v(t))\tilde{x}_2(t) \tag{16}$$

The limitation of the attack duration and attack frequency is given in the following assumptions.

Assumption 5 (39). Assume that there exists a uniform lower bound ϵ_{min} on the lengths of the DoS sleeping periods ϵ_n of the attacker, that is,

$$0 < \epsilon_{min} \leq \inf_{n \in N} \{\epsilon_n\}. \tag{17}$$

Similarly, assume that there exists a uniform upper bound c_{max} on the lengths of the DoS sleeping periods $w_{n+1} - w_n - \epsilon_n$ of the attacker, that is,

$$0 < \sup_{n \in N} \{w_{n+1} - w_n - \epsilon_n\} \leq c_{max} < \infty. \tag{18}$$

where ϵ_{min} and c_{max} are positive constants.

Assumption 6 (40). For any $m \in [0, t_1]$, the frequency of DoS attacks $\mathcal{F}(\cdot)$ over $[m, t_1)$ satisfies

$$\mathcal{F}(\cdot) \leq \mathcal{T}_0 + \frac{t_1 - m}{m_D} \tag{19}$$

where $\mathcal{T}_0 > 0$ and $m_D > 0$, $\mathcal{F}(\cdot)$ represents the number of DoS off/on transitions over $[m, t_1)$, $\mathcal{F}(\cdot) = card\{n \in \mathbb{N} | w_n + \epsilon_n \in [m, t_1)\}$, *card* represents the number of elements in the set.

Remark 5. In this article, a complex cyber-attacks model is established by considering replay attacks, deception attacks and DoS attacks in order. It needs to declare that other sequences of complex cyber-attacks also can be modeled with the same method.

2.5 | Controller design

In this article, we assume that the whole time of nonperiodic DoS attacks can be divided into two set, namely, $\mathcal{M}_n$ and $\mathcal{N}_n$. $\mathcal{M}_n$ denotes DoS attacks sleeping intervals; and $\mathcal{N}_n$ represents DoS attacks active intervals. Considering the impact of DoS attacks, we improve the ETS and the triggering instants are described as

$$t_{k,n}h = \{t_{k,n}h \quad satisfying \quad (3) | t_{k,n}h \in \mathcal{M}_{n-1}\} \cup \{w_n\}$$

where $n \in \mathbb{N}$, k represents the number of event triggering times during the n_{th} jammer action period, and $k \in \{0, 1, \ldots, k(n)\} \triangleq \phi(n)$. $k(n) = sup\left\{w_n + \epsilon_n \geq t_{k,n+1}h\right\}$.

Define $\mathcal{R}_{k,n} \triangleq [t_{k,n}h, t_{k+1,n}h)$, $\zeta_{k,n} \triangleq sup\{t_{k+1,n}h > t_{k,n}h + qh, q = 1, 2, \ldots, \hat{q}\}$.

The time interval $\mathcal{R}_{k,n}$ can be divided as

$$\mathcal{R}_{k,n} = \cup_{q=1}^{\zeta_{k,n}} \mathcal{W}_{k,n}^{q} \tag{20}$$

where

$$\begin{cases} \mathcal{W}_{k,n}^{q} = [t_{k,n}h + (q-1)h, t_{k,n}h + qh), \\ q \in \{1, \ldots, \zeta_{k,n}\} \\ \mathcal{W}_{k,n}^{\zeta_{k,n}+1} = [t_{k,n}h + \zeta_{k,n}h, t_{k+1,n}h) \end{cases} \tag{21}$$

Note that

$$\mathcal{M}_n = \cup_{k=1}^{k(n)} \{\mathcal{R}_{k,n} \cap \mathcal{M}_n\} \subseteq \cup_{k=1}^{k(n)} \mathcal{R}_{k,n} \tag{22}$$

On the basis of (20)–(22), the time interval can be expressed as

$$\mathcal{M}_n = \cup_{k=1}^{k(n)} \cup_{q=1}^{\zeta_{k,n}} \{\mathcal{W}_{k,n}^{q} \cap \mathcal{M}_n\} \tag{23}$$

Let $G_{k,n}^{q} = \{\mathcal{W}_{k,n}^{q} \cap \mathcal{M}_n\}$, and then one can get $\mathcal{M}_n = \cup_{k=1}^{k(n)} \cup_{q=1}^{\zeta_{k,n}} G_{k,n}^{q}$. Thus, for $n \in N$, $k \in \phi(n)$, two piecewise functions can be derived as follows

$$\tau_{k,n}(t) = \begin{cases} t - t_{k,n}h, t \in G_{k,n}^{1} \\ t - t_{k,n}h - h, t \in G_{k,n}^{2} \\ \vdots \\ t - t_{k,n}h - (\zeta_{k,n} - 1)h, t \in G_{k,n}^{\zeta_{k,n}} \end{cases}$$

and

$$e_{k,n}(t) = \begin{cases} 0, t \in G_{k,n}^{1} \\ x(t_{k,n}h) - x(t_{k,n}h + h), t \in G_{k,n}^{2} \\ \vdots \\ x(t_{k,n}h) - x(t_{k,n}h - \zeta_{k,n}h, t \in G_{k,n}^{\zeta_{k,n}} \end{cases}$$

Based on the above two functions, it can be acquired that $\tau_{k,n}(t) \in [0, \tau_M)$, $t \in \mathcal{R}_{k,n} \cap \mathcal{M}_n$.

The signal delivered into the communication network can be described as

$$x(t_{k,n}h) = x(t - \tau_{k,n}(t)) + e_{k,n}(t) \tag{24}$$

Combining the equalities (2), (7), (11), (12), (13), and (16), one can derive the real input of controller

$$u(t)=\begin{cases}K\left\{\varrho(t)f(x(t-d(t)))+(1-\varrho(t))[(1-\varepsilon(t))(I+\Delta_r)(x(t-\tau(t))+e_k(t))\right.\\ \quad\left.+\varepsilon(t)x_r(t)]\right\},t\in\mathcal{R}_{k,n}\cap\mathcal{M}_n\\ 0,\quad t\in\mathcal{N}_n\end{cases}\tag{25}$$

By substituting (25) into (1), we can obtain the following:

$$\dot{x}(t)=\begin{cases}Ax(t)+BK\varrho(t)f(x(t-d(t)))+Eg(x(t-\eta(t)))+BK(1-\varrho(t))[\varepsilon(t)x_r(t)\\ +(1-\varepsilon(t))(I+\Delta_r)(x(t-\tau(t))+e_k(t))],t\in\mathcal{R}_{k,n}\cap\mathcal{M}_n\\ Ax(t)+Eg(x(t-\eta(t))),\quad t\in\mathcal{N}_n\\ \lambda(t),t\in[-h,0)\end{cases}\tag{26}$$

Before giving main results, some lemmas are introduced as follows.

Lemma 1 (38). *For all of constant matrices $W\in\mathbb{R}^{n\times n}$ and $V\in\mathbb{R}^{n\times n}$ satisfying $\begin{bmatrix}W & *\\ V & W\end{bmatrix}\geq 0$, the following inequality holds:*

$$-\tilde{\tau}\int_{t-\tilde{\tau}}^{t}\dot{x}^T(s)W\dot{x}(s)ds\leq\begin{bmatrix}x(t)\\ x(t-\tau(t))\\ x(t-\tilde{\tau})\end{bmatrix}^T\begin{bmatrix}-W & * & *\\ W-V & -2W+V+V^T & *\\ V & W-V & -W\end{bmatrix}\begin{bmatrix}x(t)\\ x(t-\tau(t))\\ x(t-\tilde{\tau})\end{bmatrix}$$

where $\tau(t)$ satisfies $0\leq\tau(t)\leq\tilde{\tau}$.

Lemma 2 (41). *For given appropriately dimensioned matrices H_1, H_2 and a symmetric matrix A, the inequality $A+sym\{H_1\Delta H_2\}<0$ holds for all Δ satisfying $\Delta^T\Delta\leq I$ if and only if there exist a positive scalar $d_1>0$ such that $A+d_1H_1^TH_1+d_1^{-1}H_2^TH_2<0$.*

Lemma 3 (42). *For $x(t)$ and $g(x(t))$, there exists a semi-definite diagonal matrix M satisfying the following inequality.*

$$\begin{bmatrix}x(t)\\ g(x(t))\end{bmatrix}^T\begin{bmatrix}-M\Gamma_g^- & M\Gamma_g^+\\ \Gamma_g^+M & -M\end{bmatrix}\begin{bmatrix}x(t)\\ g(x(t))\end{bmatrix}\geq 0\tag{27}$$

where $\Gamma_g^-=diag\{\gamma_{g1}^-\gamma_{g1}^+,\gamma_{g2}^-\gamma_{g2}^+,\ \dots\ ,\gamma_{gn}^-\gamma_{gn}^+\}$ and $\Gamma_g^+=diag\left\{\frac{\gamma_{g1}^-+\gamma_{g1}^+}{2},\frac{\gamma_{g2}^-+\gamma_{g2}^+}{2},\ \dots\ ,\frac{\gamma_{gn}^-+\gamma_{gn}^+}{2}\right\}$.

3 | MAIN RESULTS

Theorem 1. *For given positive scalars ρ_i, $a_i(i=1,2)$, $\overline{\varepsilon}$, $\overline{\varrho}$, d_M, η_M, τ_M, sampling period h, quantized parameter r, trigger parameter σ, DoS parameters c_{max}, ϵ_{min}, m_D, $\mathcal{T}_0$, the matrices K and F, the system is exponentially mean-square stable if there exist matrices $H_i>0$, $J_i>0$, $R_i>0$, $Z_i>0$, $S_i>0$, $P_i>0$, $Q_i>0$, U_i, W_i, M_i, N_i, $V_i(i=1,2)$ and $\Omega>0$ with compatible dimensions satisfying the following inequalities.*

$$\Psi^i=\begin{bmatrix}\Upsilon_{11}^i & * & * & * & *\\ \Upsilon_{21}^i & \Upsilon_{22}^i & * & * & *\\ \Upsilon_{31}^i & \Upsilon_{32}^i & \Upsilon_{33}^i & * & *\\ \Upsilon_{41}^i & \Upsilon_{42}^i & 0 & \Upsilon_{44}^i & *\\ \Upsilon_{51}^i & \Upsilon_{52}^i & 0 & 0 & \Upsilon_{55}^i\end{bmatrix}<0\tag{28}$$

$$P_1\leq a_2P_2,P_2\leq a_1e^{2(\rho_1+\rho_2)h}P_1\tag{29}$$

$$\begin{cases} Q_1 \le a_2 Q_2, Q_2 \le a_1 Q_1 \\ R_1 \le a_2 R_2, R_2 \le a_1 R_1 \\ Z_1 \le a_2 Z_2, Z_2 \le a_1 Z_1 \end{cases} \tag{30}$$

$$s = \frac{2\rho_1(\epsilon_{min} - h) - 2\rho_2(h + c_{max}) - \ln(a_1 a_2)}{m_D} > 0 \tag{31}$$

where the elements of matrix Ψ^i are given in Appendix A.

Proof. See Appendix B. ■

Sufficient conditions, which can ensure the exponential mean-square stability of the system, are acquired in Theorem 1. Based on the results in Theorem 1, the algorithm of controller design is given for neural networks in Theorem 2.

Theorem 2. *For given positive scalars ρ_i, a_i, e_{i1}, e_{i2}, $e_{i3} (i = 1, 2)$, $\overline{\varepsilon}$, $\overline{\varrho}$, d_M, η_M, τ_M, sampling period h, quantized parameter r, trigger parameter σ, DoS parameters c_{max}, ϵ_{min}, m_D, $\mathcal{T}_0$, the matrices F, the system is exponentially mean-square stable if there exist matrices $\hat{Q}_i > 0$, $\hat{H}_i > 0$, $\hat{J}_i > 0$, $\hat{R}_i > 0$, $\hat{Z}_i > 0$, $\hat{S}_i > 0$, $X_i > 0$, $\hat{\Omega} > 0$, $\hat{U}_i$, $\hat{W}_i$, $\hat{M}_i$, $\hat{N}_i$, $\hat{V}_i (i = 1, 2)$, Y with compatible dimensions, such that for i = 1, 2 the following linear matrix inequalities and condition (31) hold:*

$$\hat{\Psi}^i = \begin{bmatrix} \hat{\Upsilon}^i_{11} & * & * & * & * \\ \hat{\Upsilon}^i_{21} & \hat{\Upsilon}^i_{22} & * & * & * \\ \hat{\Upsilon}^i_{31} & \hat{\Upsilon}^i_{32} & \hat{\Upsilon}^i_{33} & * & * \\ \hat{\Upsilon}^i_{41} & \hat{\Upsilon}^i_{42} & 0 & \hat{\Upsilon}^i_{44} & * \\ \hat{\Upsilon}^i_{51} & \hat{\Upsilon}^i_{52} & 0 & 0 & \hat{\Upsilon}^i_{55} \end{bmatrix} < 0 \tag{32}$$

$$\begin{bmatrix} -a_2 X_2 & * \\ X_2 & -X_1 \end{bmatrix} \le 0 \tag{33}$$

$$\begin{bmatrix} -a_1 e^{2(\rho_1+\rho_2)h} X_2 & * \\ X_1 & -X_2 \end{bmatrix} \le 0 \tag{34}$$

$$\begin{bmatrix} -a_{3-i}\hat{Q}_{3-i} & * \\ X_{3-i} & e_{i1}^2 \hat{Q}_i - 2e_{i1}X_i \end{bmatrix} \le 0 \tag{35}$$

$$\begin{bmatrix} -a_{3-i}\hat{R}_{3-i} & * \\ X_{3-i} & e_{i2}^2 \hat{R}_i - 2e_{i2}X_i \end{bmatrix} \le 0 \tag{36}$$

$$\begin{bmatrix} -a_{3-i}\hat{Z}_{3-i} & * \\ X_{3-i} & e_{i3}^2 \hat{Z}_i - 2e_{i3}X_i \end{bmatrix} \le 0 \tag{37}$$

where the elements of matrix $\hat{\Psi}^i$ are given in Appendix C.

In addition, the desired controller gain is derived as follows

$$K = YX_1^{-1} \tag{38}$$

Proof. See Appendix D. ■

4 | NUMERICAL EXAMPLE

In this section, a numerical example is presented to demonstrate the effectiveness of proposed method.

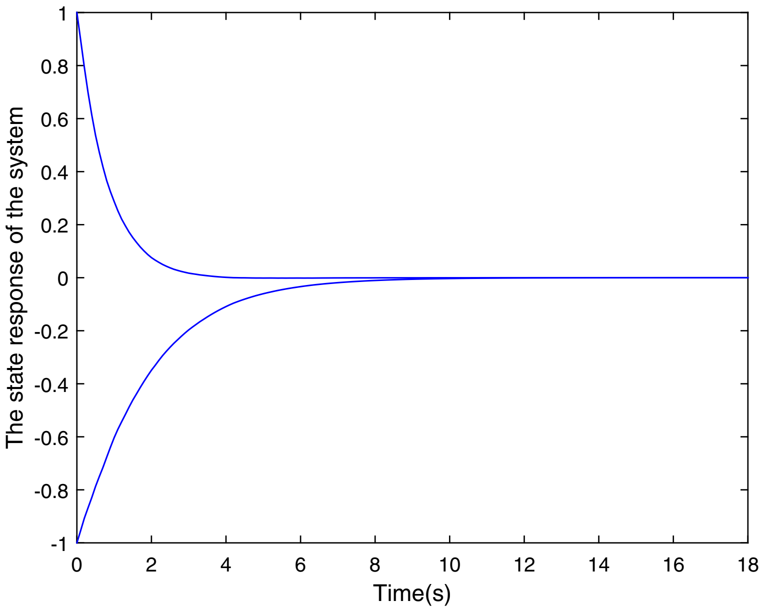

FIGURE 4 The state response of the system in case 1 [Colour figure can be viewed at wileyonlinelibrary.com]

Considering the system (1) with following parameters:

$$A = \begin{bmatrix} -0.6 & 0 \\ 0 & -0.5 \end{bmatrix}, B = \begin{bmatrix} 0.1 & 0.1 \\ 0.2 & 0.1 \end{bmatrix}, E = \begin{bmatrix} 0.1 & -0.2 \\ 0.05 & -0.92 \end{bmatrix}, C = \begin{bmatrix} 0.1 & 0.1 \\ 0.1 & 0.1 \end{bmatrix}$$

The neuron activation function is defined as $g(x(t)) = [tanh(0.04x_1(t)) \quad tanh(0.04x_2(t))]^T$, and one can obtain $\Gamma_g^- = \text{diag}\{0, 0\}$, $\Gamma_g^+ = \text{diag}\{0.02, 0.02\}$. The deception attack function is chosen as $f(x(t)) = [tanh(0.25x_1(t)) \quad tanh(0.15x_2(t))]^T$, which can satisfy the inequality (14) in Assumption 4 with $F = \text{diag}\{0.15, 0.25\}$. And it can be acquired $\Gamma_f^- = \text{diag}\{0, 0\}$, $\Gamma_f^+ = \text{diag}\{0.125, 0.075\}$.

In the following, two cases are discussed to testify the feasibility of desired controller. In Case 1, the complex cyber-attacks are not considered. Case 2 shows the performance of the quantized controller under complex cyber-attacks.

Case 1:

Setting $\bar{\epsilon} = 0$, $\bar{\varrho} = 0$, it means that the complex cyber-attacks do not occur. Set $d_M = 0.01$, $\eta_M = 0.12$, $\tau_M = 0.04$, $h = 0.1s$, $\sigma = 0.2$, $e_1 = e_2 = 1$, the quantizer parameter $r = 0.818$. By solving Theorem 2 with MATLAB, the following matrices can be acquired

$$X_1 = \begin{bmatrix} 0.0422 & 0.0004 \\ 0.0004 & 0.0261 \end{bmatrix}, Y = \begin{bmatrix} 0.0122 & -0.0103 \\ -0.0103 & 0.0185 \end{bmatrix}, \Omega = \begin{bmatrix} 75.2960 & -0.0417 \\ -0.0417 & 75.4735 \end{bmatrix}$$

According to the equality (38) in Theorem 2, one can get the controller gain

$$K = \begin{bmatrix} 0.2929 & -0.2503 \\ -0.3984 & 0.7125 \end{bmatrix}$$

Set the initial system condition as $x = \begin{bmatrix} -1 & 1 \end{bmatrix}^T$. The simulation results are shown in Figures 4 to 6. The state trajectory of neural networks without cyber-attacks is exhibited in Figure 4. In Figure 5, the red line denotes the normal signal without quantization, and the blue line represents the quantized signal. The triggering instants and the releasing intervals of AETS are given in Figure 6. According to above graphs, Case 1 shows the usefulness of the desired controller for neural networks without complex cyber-attacks.

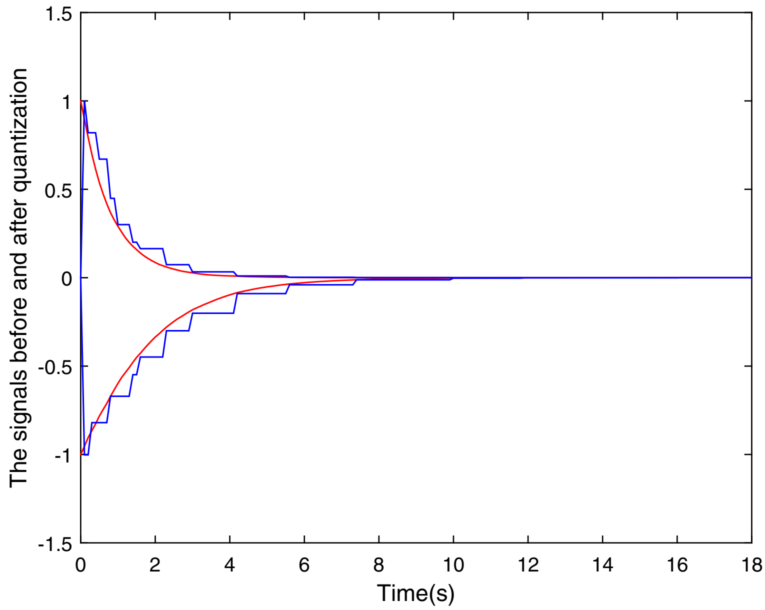

FIGURE 5 The signals before and after quantization in case 1 [Colour figure can be viewed at wileyonlinelibrary.com]

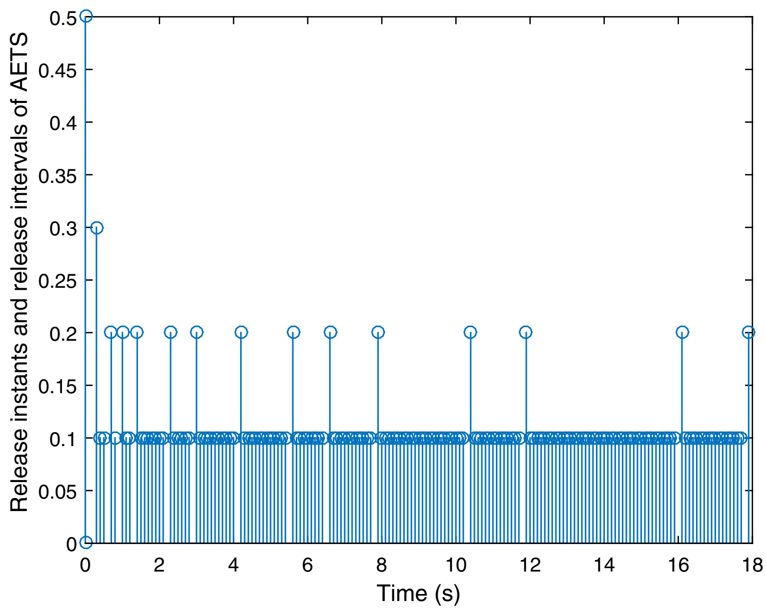

FIGURE 6 Release instants and intervals of AETS in case 1 [Colour figure can be viewed at wileyonlinelibrary.com]

Case 2:

Setting $\overline{\varepsilon} = 0.3$, $\overline{\varrho} = 0.4$, $\epsilon_{min} = 1.78$, $c_{max} = 0.2$, it denotes that the complex cyber-attacks are considered. Set $d_M = 0.01$, $\eta_M = 0.12$, $\tau_M = 0.04$, $h = 0.1s$, $\sigma = 0.2$, $e_1 = e_2 = 1$, $a_1 = a_2 = 1.05$, $\rho_1 = 0.1$, $\rho_2 = 0.15$, $\mathcal{T}_0 = 1$, $m_D = 4$, the quantizer parameter $r = 0.818$, and Table 1 shows the DoS-related parameters. With the above parameters, the following matrices are obtained by solving Theorem 2 through MATLAB.

$$X_1 = \begin{bmatrix} 0.0196 & 0.0001 \\ 0.0001 & 0.0141 \end{bmatrix}, Y = \begin{bmatrix} 0.0071 & -0.0185 \\ -0.0185 & 0.0172 \end{bmatrix}, \Omega = \begin{bmatrix} 35.0782 & -0.0053 \\ -0.0053 & 35.1422 \end{bmatrix}$$

Based on the equality (38) in Theorem 2, the controller gain can be acquired

$$K = \begin{bmatrix} 0.3641 & -0.9405 \\ -1.3085 & 1.2223 \end{bmatrix}$$

TABLE 1 DoS-related parameter in case 2

0	n = 0	n =1	n=2	n=3	n=4	n=5
ϵ_n	0	2.58	3.07	3.34	3.14	3.77
$w_{n+1} - w_n - \epsilon_n$	0	0.11	0.15	0.14	0.12	0.10
w_n	0	2.69	5.91	9.39	12.65	16.52

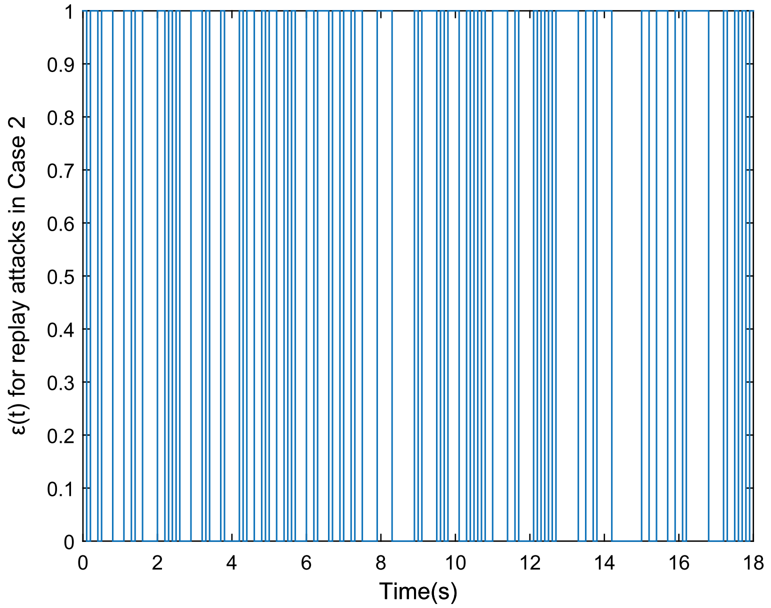

FIGURE 7 The Bernoulli distribution variables of $\varepsilon(t)$ in case 2 [Colour figure can be viewed at wileyonlinelibrary.com]

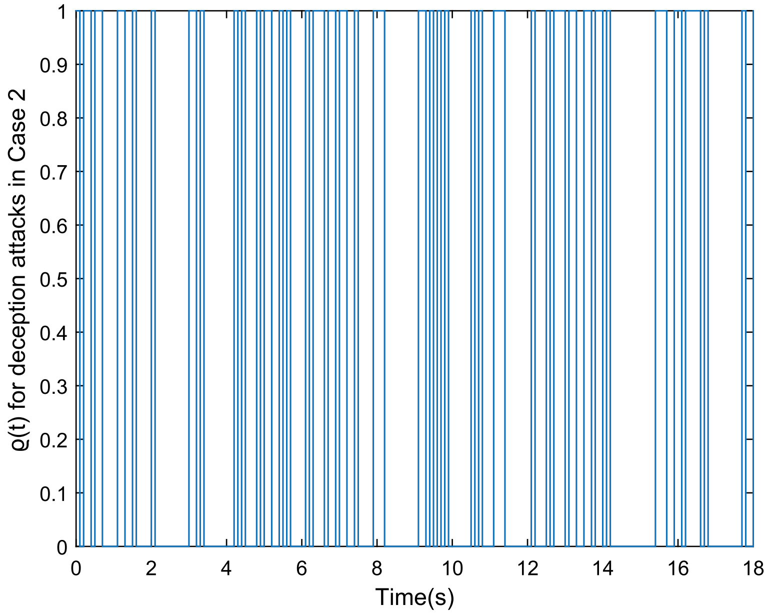

FIGURE 8 The Bernoulli distribution variables of $\varrho(t)$ in case 2 [Colour figure can be viewed at wileyonlinelibrary.com]

Set the initial system condition as $x = \begin{bmatrix} -1 & 1 \end{bmatrix}^T$. The following graphs Figure 7 to 11 can be obtained by MATLAB simulation. Figures 7 and 8 present the Bernoulli distribution variables for replay attacks and deception attacks, respectively. Figure 9 shows nonperiodic DoS jamming signal. Figure 10 exhibits the signal subjected to replay attacks and deception attacks. The state response of neural networks is exhibited in Figure 11, which shows that the closed-loop system with complex cyber-attacks is stable. According to the graphs above, it can be concluded that the proposed controller for neural networks with complex cyber-attacks is feasible.

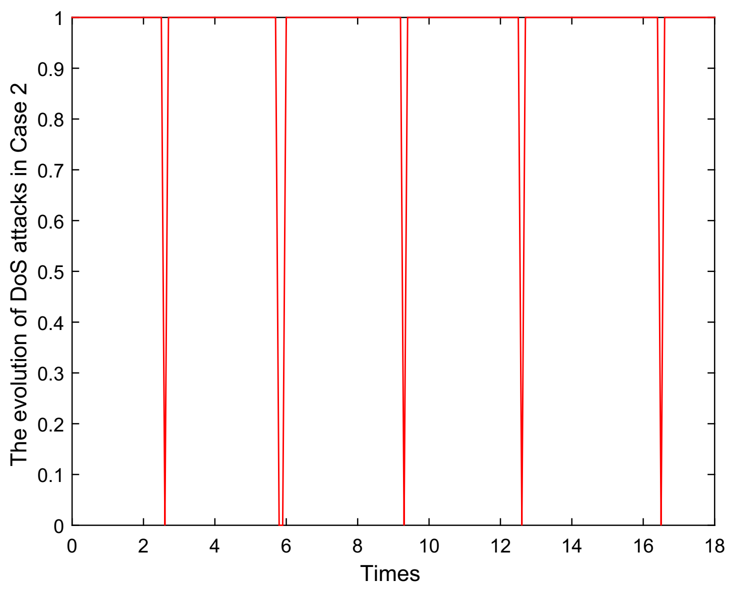

FIGURE 9 The DoS attacks jamming signal intervals [Colour figure can be viewed at wileyonlinelibrary.com]

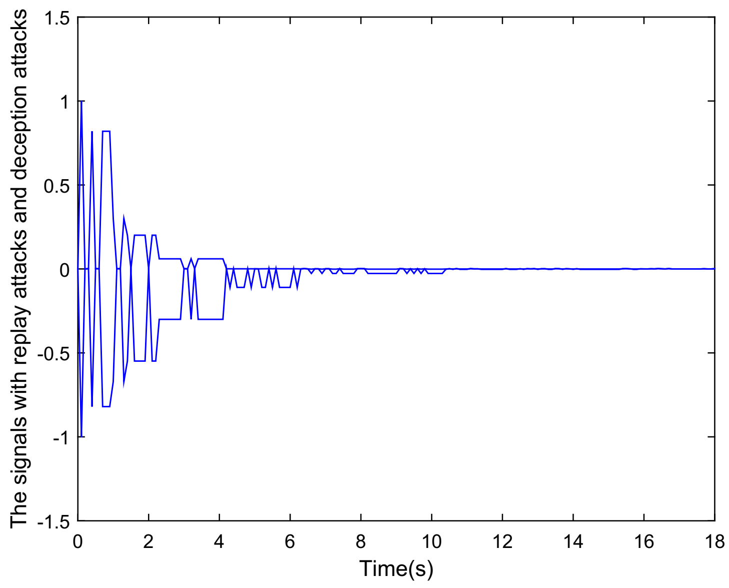

FIGURE 10 The transmitted signal under replay attacks and deception attacks [Colour figure can be viewed at wileyonlinelibrary.com]

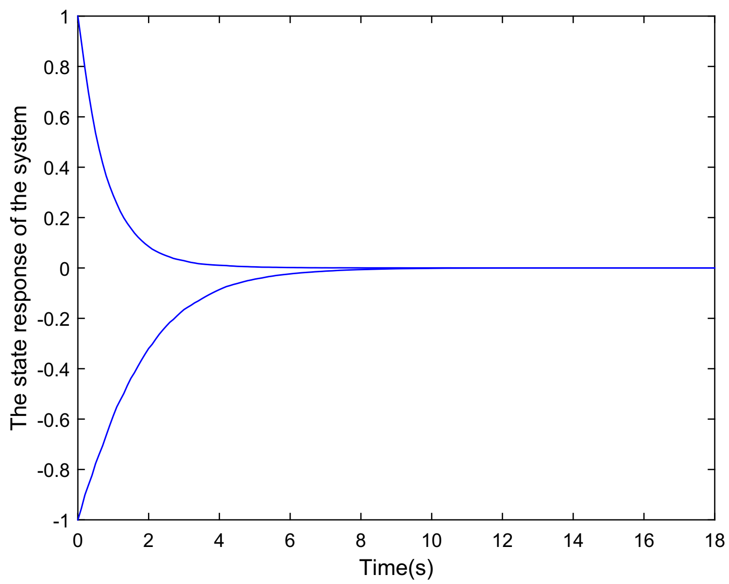

FIGURE 11 The state response of the system in case 2 [Colour figure can be viewed at wileyonlinelibrary.com]

5 CONCLUSION

This article focuses on the quantized control for neural networks with AETS and complex cyber-attacks. A mathematical model of complex cyber-attacks is firstly built for neural networks. A quantization mechanism and an AETS are employed to mitigate the burden of network transmission. Then the sufficient conditions, which can ensure the stability of closed-loop system, are derived by utilizing Lyapunov stability theory. Moreover, the controller gain can be acquired by solving a series of linear matrix inequalities. At last, a simulation example is presented to verify the feasibility of proposed method. In the future, we will study the detection and isolation of the cyber-attacks for neural networks.

ACKNOWLEDGMENTS

This work was supported in part by the National Natural Science Foundation of China under Grant 61973152 and Grant 61903182, in part by the Natural Science Foundation of Jiangsu Province of China under Grant BK20190794, in part by the major project supported by the Natural Science Foundation of the Jiangsu Higher Education Institutions of China under Grant 19KJA510005, in part by the Fundamental Research Funds for the Central Universities under Grant No.3091901140, and in part by the Qing Lan Project.

DATA AVAILABILITY STATEMENT

Data sharing not applicable to this article as no datasets were generated or analyzed during the current study.

ORCID

Jinliang Liu https://orcid.org/0000-0001-5489-0246

REFERENCES

1. Zhai J, Karimi HR. Global output feedback control for a class of nonlinear systems with unknown homogenous growth condition. *Int J Robust Nonlinear Control*. 2019;29(7):2082-2095.
2. Liang H, Zhang L, Karimi HR, Zhou Q. Fault estimation for a class of nonlinear semi-Markovian jump systems with partly unknown transition rates and output quantization. *Int J Robust Nonlinear Control*. 2018;28(18):5962-5980.
3. Du D, Jiang B, Shi P, Karimi HR. Fault detection for continuous-time switched systems under asynchronous switching. *Int J Robust Nonlinear Control*. 2014;24(11):1694-1706.
4. Ma H, Li H, Lu R, Huang T. Adaptive event-triggered control for a class of nonlinear systems with periodic disturbances. *Sci China Inf Sci*. 2020;63:1-15.
5. Wu C, Wu L, Liu J, Jiang Z. Active defense-based resilient sliding mode control under denial-of-service attacks. *IEEE Trans Inf Forens Secur*. 2019;15:237-249.
6. Wu Z, Karimi HR, Dang C. An approximation algorithm for graph partitioning via deterministic annealing neural network. *Neural Netw*. 2019;117:191-200.
7. Zhou N, Chen R, Xia Y, Huang J, Wen G. Neural network-based reconfiguration control for spacecraft formation in obstacle environments. *Int J Robust Nonlinear Control*. 2018;28(6):2442-2456.
8. Rajchakit G, Saravanakumar R, Ahn CK, Karimi HR. Improved exponential convergence result for generalized neural networks including interval time-varying delayed signals. *Neural Netw*. 2017;86:10-17.
9. Saravanakumar R, Kang HS, Ahn CK, Su X, Karimi HR. Robust stabilization of delayed neural networks: dissipativity-learning approach. *IEEE Trans Neural Netw Learn Syst*. 2019;30(3):913-922.
10. Ali MS, Saravanakumar R, Ahn CK, Karimi HR. Stochastic H_∞ filtering for neural networks with leakage delay and mixed time-varying delays. *Inf Sci*. 2017;388-389:118-134.
11. Li Z, Xia Y. Adaptive neural network control of bilateral teleoperation with unsymmetrical stochastic delays and unmodeled dynamics. *Int J Robust Nonlinear Control*. 2014;24(11):1628-1652.
12. Shi Y, Tian E, Shen S, Zhao X. Adaptive memory-event-triggered H-infinity control for network-based T-S fuzzy systems with asynchronous premise constraints. *IET Control Theory Appl*. 2021;15:534-544.
13. Gu Z, Ahn CK, Yue D, Xie X. Event-triggered H_∞ filtering for T–S fuzzy-model-based nonlinear networked systems with multi-sensors against DoS attacks. *IEEE Trans Cybern*. 2020. https://doi.org/10.1109/TCYB.2020.3030028.
14. Wang K, Tian E, Liu J, Wei L, Yue D. Resilient control of networked control systems under deception attacks: a memory-event-triggered communication scheme. *Int J Robust Nonlinear Control*. 2020;30(4):1534-1548.
15. Gu Z, Shi P, Yue D, Yan S, Xie X. Memory-based continuous event-triggered control for networked T-S fuzzy systems against cyber-attacks. *IEEE Trans Fuzzy Syst*. 2020. https://doi.org/10.1109/TFUZZ.2020.3012771.
16. Yue D, Tian E, Han Q. A delay system method for designing event-triggered controllers of networked control systems. *IEEE Trans Autom Control*. 2013;58(2):475-481.
17. Cao J, Ding D, Liu J, Tian E, Hu S, Xie X. Hybrid-triggered-based security controller design for networked control system under multiple cyber attacks. *Inf Sci*. 2021;548:69-84.

18. Liu J, Suo W, Zha L, Tian E, Xie X. Security distributed state estimation for nonlinear networked systems against denial-of-service attacks. *Int J Robust Nonlinear Control*. 2020;30(3):1156-1180.
19. Liu J, Yin T, Cao J, Yue D, Reza Karimi H. Security control for T-S fuzzy systems with adaptive event-triggered mechanism and multiple cyber-attacks. *IEEE Trans Syst Man Cybern Syst*. 2019. https://doi.org/10.1109/TSMC.2019.2963143.
20. Wang Y, Karimi HR, Yan H. An adaptive event-triggered synchronization approach for chaotic Lure systems subject to aperiodic sampled data. *IEEE Trans Circuits Syst II Exp Briefs*. 2019;66(3):442-446.
21. Liu J, Wang Y, Cao J, Yue D, Xie X. Secure adaptive-event-triggered filter design with input constraint and hybrid cyber-attack. *IEEE Trans Cybern*. 2020. https://doi.org/10.1109/TCYB.2020.3003752.
22. Zhang Y, Li H, Sun J, He W. Cooperative adaptive event-triggered control for multi-agent systems with actuator failures. *IEEE Trans Syst Man Cybern Syst*. 2019;49(9):1759-1768. https://doi.org/10.1109/TSMC.2018.2883907.
23. Li H, Zhang Z, Yan H, Xie X. Adaptive event-triggered fuzzy control for uncertain active suspension systems. *IEEE Trans Cybern*. 2019;49(12):4388–4397. https://doi.org/10.1109/TCYB.2018.2864776.
24. Gu Z, Shi P, Yue D, Ding Z. Decentralized adaptive event-triggered H_∞ filtering for a class of networked nonlinear interconnected systems. *IEEE Trans Cybern*. 2019;49(5):1570-1579.
25. Wan Y, Cao J, Wen G. Quantized synchronization of chaotic neural networks with scheduled output feedback control. *IEEE Trans Neural Netw Learn Syst*. 2017;28(11):2638-2647.
26. Che W, Wang J, Yang G. Quantized H_∞ filtering for networked systems with random sensor packet losses. *IET Control Theory Appl*. 2010;4(8):1339-1352.
27. Lu R, Tao J, Shi P, Su H, Wu Z, Xu Y. Dissipativity-based resilient filtering of periodic Markovian jump neural networks with quantized measurements. *IEEE Trans Neural Netw Learn Syst*. 2018;29(5):1888-1899.
28. Fan Q, Yang G, Ye D. Quantization-based adaptive actor-critic tracking control with tracking error constraints. *IEEE Trans Neural Netw Learn Syst*. 2018;29(4):970-980.
29. Liu S, Wei G, Song Y, Liu Y. Error-constrained reliable tracking control for discrete time-varying systems subject to quantization effects. *Neurocomputing*. 2016;174:897-905.
30. Tian E, Yue D, Peng C. Quantized output feedback control for networked control systems. *Inf Sci*. 2008;178(12):2734-2749.
31. Cheng J, Park JH, Cao J, Zhang D. Quantized H_∞ filtering for switched linear parameter-varying systems with sojourn probabilities and unreliable communication channels. *Inf Sci*. 2018;466:289-302.
32. Yang Y, Yue D, Xu C. Dynamic event-triggered leader-following consensus control of a class of linear multi-agent systems. *J Frankl Inst*. 2018;355(15):7706-7734.
33. Hao L, Park JH, Ye D. Integral sliding mode fault-tolerant control for uncertain linear systems over networks with signals quantization. *IEEE Trans Neural Netw Learn Syst*. 2017;28(9):2088-2100.
34. Ding D, Han Q, Xiang Y, Ge X, Zhang X. A survey on security control and attack detection for industrial cyber-physical systems. *Neurocomputing*. 2018;275:1674-1683.
35. Liu J, Wu Z, Yue D, Park JH. Stabilization of networked control systems with hybrid-driven mechanism and probabilistic cyber-attacks. *IEEE Trans Syst Man Cybern Syst*. 2021;51(2):943-953.
36. Chen X, Wang Y, Hu S. Event-based robust stabilization of uncertain networked control systems under quantization and denial-of-service attacks. *Inf Sci*. 2018;459:369-386.
37. Chen X, Wang Y, Hu S. Event-triggered quantized H_∞ control for networked control systems in the presence of denial-of-service jamming attacks. *Nonlinear Anal Hybrid Syst*. 2019;33:265-281.
38. Gu Z, Yue D, Tian E. On designing of an adaptive event-triggered communication scheme for nonlinear networked interconnected control systems. *Inf Sci*. 2018;422:257-270.
39. Sun Y, Yang G. Event-triggered resilient control for cyber-physical systems under asynchronous DoS attacks. *Inf Sci*. 2018;465:340-352.
40. Zhi F, Wen G, Hu G. Distributed secure coordinated control for multiagent systems under strategic attacks. *IEEE Trans Cybern*. 2017;47(5):1273-1284.
41. Liu J, Yin T, Yue D, Reza Karimi H, Cao J. Event-based secure leader-following consensus control for multi-agent systems with multiple cyber-attacks. *IEEE Trans Cybern*. 2021;51(1):162-173.
42. Zha L, Tian E, Xie X, Gu Z, Cao J. Decentralized event-triggered H_∞ control for neural networks subject to cyber-attacks. *Inf Sci*. 2018;457:141-155.

How to cite this article: Liu J, Suo W, Xie X, Yue D, Cao J. Quantized control for a class of neural networks with adaptive event-triggered scheme and complex cyber-attacks. *Int J Robust Nonlinear Control*. 2021;31:4705–4728. https://doi.org/10.1002/rnc.5500

APPENDIX A. THE ELEMENTS OF THEOREM 1

$$\Psi^1 = \begin{bmatrix} \Upsilon_{11}^1 & * & * & * & * \\ \Upsilon_{21}^1 & \Upsilon_{22}^1 & * & * & * \\ \Upsilon_{31}^1 & \Upsilon_{32}^1 & \Upsilon_{33}^1 & * & * \\ \Upsilon_{41}^1 & \Upsilon_{42}^1 & 0 & \Upsilon_{44}^1 & * \\ \Upsilon_{51}^1 & \Upsilon_{52}^1 & 0 & 0 & \Upsilon_{55}^1 \end{bmatrix}$$

$$\Upsilon_{11}^1 = \begin{bmatrix} \Theta_{11}^1 & * & * & * & * & * & * & * \\ \Theta_{21}^1 & \Theta_{22}^1 & * & * & * & * & * & * \\ \Theta_{31}^1 & \Theta_{32}^1 & \Theta_{33}^1 & * & * & * & * & * \\ \Theta_{41}^1 & 0 & 0 & \Theta_{44}^1 & * & * & * & * \\ \Theta_{51}^1 & 0 & 0 & \Theta_{54}^1 & \Theta_{55}^1 & * & * & * \\ \Theta_{61}^1 & 0 & 0 & 0 & 0 & \Theta_{66}^1 & * & * \\ \Theta_{71}^1 & 0 & 0 & 0 & 0 & \Theta_{76}^1 & \Theta_{77}^1 & * \\ \Theta_{81}^1 & 0 & 0 & 0 & 0 & 0 & 0 & -\Omega \end{bmatrix}$$

$$\Theta_{11}^1 = 2\rho_1 P_1 + P_1 A + A^T P_1 + Q_1 + H_1 + J_1 - f_1 R_1 - f_2 Z_1 - f_3 S_1, f_1 = e^{-2\rho_1 d_M}$$
$$\Theta_{21}^1 = f_1(R_1^T - U_1^T), f_2 = e^{-2\rho_1 \eta_M}, \Theta_{22}^1 = f_1(-2R_1 + U_1^T + U_1) - N_1 \Gamma_f^- + F^T F$$
$$\Theta_{31}^1 = f_1 U_1^T, \Theta_{32}^1 = f_1(R_1^T - U_1^T), \Theta_{33}^1 = f_1(Q_1 - R_1), f_3 = e^{-2\rho_1 \tau_M}$$
$$\Theta_{41}^1 = f_2(Z_1^T - W_1^T), \Theta_{44}^1 = f_2(-2Z_1 + W_1 + W_1^T) - M_1 \Gamma_g^-, \Theta_{51}^1 = f_2 W_1$$
$$\Theta_{54}^1 = f_2(Z_1^T - W_1^T), \Theta_{55}^1 = f_2(H_1 - Z_1), \Theta_{66}^1 = f_3(-2S_1 + L_1 + L_1^T), \overline{\varrho}_1 = 1 - \overline{\varrho}$$
$$\Theta_{61}^1 = (I + \Delta_r)\overline{\varrho}_1 \overline{\varepsilon}_1 K^T B^T P_1 + f_3 S_1 - f_3 L_1, \Theta_{71}^1 = f_3 L_1^T, \Theta_{76}^1 = f_3(S_1^T - L_1^T)$$
$$\Theta_{77}^1 = f_3(J_1 - S_1), \Theta_{81}^1 = (I + \Delta_r)\overline{\varrho}_1 \overline{\varepsilon}_1 K^T B^T P_1, \delta_1 = \sqrt{\overline{\varepsilon}\,\overline{\varepsilon}_1}, \delta_2 = \sqrt{\overline{\varrho}\,\overline{\varrho}_1}, \overline{\varepsilon}_1 = 1 - \overline{\varepsilon}$$

$$\Upsilon_{21}^1 = \begin{bmatrix} \overline{\varrho}\,\overline{\varepsilon}_1 K^T B^T P_1 & 0 & 0 & 0 & 0_{1\times 4} \\ \overline{\varrho}\,\overline{\varepsilon}_1 K^T B^T P_1 & 0 & 0 & 0 & 0_{1\times 4} \\ E^T P_1 & 0 & 0 & \Gamma_g^+ M_1 & 0_{1\times 4} \\ \overline{\varepsilon} K^T B^T P_1 & \Gamma_f^+ N_1 & 0 & 0 & 0_{1\times 4} \end{bmatrix}$$

$$\Upsilon_{22}^1 = diag\{\sigma\Omega, -\Omega, -M_1, -N_1\}, \Upsilon_{31}^1 = \begin{bmatrix} \Lambda_{31}^1 & \Xi_{31}^1 \end{bmatrix}, \Upsilon_{32}^1 = \begin{bmatrix} \Lambda_{32}^1 & \Xi_{32}^1 \end{bmatrix}$$

$$\Lambda_{31}^1 = \begin{bmatrix} d_M P_1 A & 0_{1\times 4} & d_M \overline{\varrho}_1 \overline{\varepsilon}_1 P_1 BK \\ 0 & 0_{1\times 4} & d_M (I + \Delta_r)\delta_1 \overline{\varepsilon}_1 P_1 BK \\ 0 & 0_{1\times 4} & d_M (I + \Delta_r)\delta_2 P_1 BK \\ 0 & 0_{1\times 4} & -d_M \delta_1 \delta_2 P_1 BK \end{bmatrix}, \Xi_{31}^1 = \begin{bmatrix} 0 & d_M \overline{\varrho}_1 \overline{\varepsilon}_1 P_1 BK \\ 0 & d_M (I + \Delta_r)\delta_1 \overline{\varepsilon}_1 P_1 BK \\ 0 & d_M (I + \Delta_r)\delta_2 P_1 BK \\ 0 & -d_M \delta_1 \delta_2 P_1 BK \end{bmatrix}$$

$$\Xi_{32}^1 = \begin{bmatrix} d_M P_1 E & d_M \overline{\varepsilon} P_1 BK \\ 0 & d_M P_1 BK \\ 0 & 0 \\ 0 & 0 \end{bmatrix}, \Lambda_{32}^1 = \begin{bmatrix} d_M \overline{\varrho}\,\overline{\varepsilon}_1 P_1 BK & d_M \overline{\varrho}\,\overline{\varepsilon}_1 P_1 BK \\ d_M \delta_1 \overline{\varepsilon}_1 P_1 BK & d_M \delta_1 \overline{\varepsilon}_1 P_1 BK \\ -d_M \delta_2 P_1 BK & -d_M \delta_2 P_1 BK \\ -d_M \delta_1 \delta_2 P_1 BK & -d_M \delta_1 \delta_2 P_1 BK \end{bmatrix}$$

$$\Upsilon_{33}^1 = diag\{-P_1 R_1^{-1} P_1, -P_1 R_1^{-1} P_1, -P_1 R_1^{-1} P_1, -P_1 R_1^{-1} P_1\}$$

$$\Upsilon_{41}^1 = \begin{bmatrix} \Lambda_{41}^1 & \Xi_{41}^1 \end{bmatrix}, \Upsilon_{42}^1 = \begin{bmatrix} \Lambda_{42}^1 & \Xi_{42}^1 \end{bmatrix}, \Upsilon_{51} = \begin{bmatrix} \Lambda_{51}^1 & \Xi_{51}^1 \end{bmatrix}, \Upsilon_{52} = \begin{bmatrix} \Lambda_{52}^1 & \Xi_{52}^1 \end{bmatrix}$$

$$\Lambda_{41}^1 = \begin{bmatrix} \eta_M P_1 A & 0_{1\times4} & \eta_M \overline{\varrho}_1 \overline{\varepsilon}_1 P_1 BK \\ 0 & 0_{1\times4} & \eta_M (I+\Delta_r)\delta_1 \overline{\varepsilon}_1 P_1 BK \\ 0 & 0_{1\times4} & \eta_M (I+\Delta_r)\delta_2 P_1 BK \\ 0 & 0_{1\times4} & -\eta_M \delta_1 \delta_2 P_1 BK \end{bmatrix}, \Xi_{41}^1 = \begin{bmatrix} 0 & \eta_M \overline{\varrho}_1 \overline{\varepsilon}_1 P_1 BK \\ 0 & \eta_M (I+\Delta_r)\delta_1 \overline{\varepsilon}_1 P_1 BK \\ 0 & \eta_M (I+\Delta_r)\delta_2 P_1 BK \\ 0 & -\eta_M \delta_1 \delta_2 P_1 BK \end{bmatrix}$$

$$\Lambda_{42}^1 = \begin{bmatrix} \eta_M \overline{\varrho} \overline{\varepsilon}_1 P_1 BK & \eta_M \overline{\varrho} \overline{\varepsilon}_1 P_1 BK \\ \eta_M \delta_1 \overline{\varepsilon}_1 P_1 BK & \eta_M \delta_1 \overline{\varepsilon}_1 P_1 BK \\ -\eta_M \delta_2 P_1 BK & -\eta_M \delta_2 P_1 BK \\ -\eta_M \delta_1 \delta_2 P_1 BK & -\eta_M \delta_1 \delta_2 P_1 BK \end{bmatrix}, \Xi_{42}^1 = \begin{bmatrix} \eta_M P_1 E & d_1 \overline{\varepsilon} P_1 BK \\ 0 & \eta_M P_1 BK \\ 0 & 0 \\ 0 & 0 \end{bmatrix}$$

$$\Upsilon_{44}^1 = diag\{-P_1 Z_1^{-1} P_1, -P_1 Z_1^{-1} P_1, -P_1 Z_1^{-1} P_1 - P_1 Z_1^{-1} P_1\}$$

$$\Lambda_{51}^1 = \begin{bmatrix} \tau_M P_1 A & 0_{1\times4} & \tau_M \overline{\varrho}_1 \overline{\varepsilon}_1 P_1 BK \\ 0 & 0_{1\times4} & \tau_M (I+\Delta_r)\delta_1 \overline{\varepsilon}_1 P_1 BK \\ 0 & 0_{1\times4} & \tau_M (I+\Delta_r)\delta_2 P_1 BK \\ 0 & 0_{1\times4} & -\tau_M \delta_1 \delta_2 P_1 BK \end{bmatrix}, \Xi_{51}^1 = \begin{bmatrix} 0 & \tau_M \overline{\varrho}_1 \overline{\varepsilon}_1 P_1 BK \\ 0 & \tau_M (I+\Delta_r)\delta_1 \overline{\varepsilon}_1 P_1 BK \\ 0 & \tau_M (I+\Delta_r)\delta_2 P_1 BK \\ 0 & -\tau_M \delta_1 \delta_2 P_1 BK \end{bmatrix}$$

$$\Lambda_{52}^1 = \begin{bmatrix} \tau_M \overline{\varrho} \overline{\varepsilon}_1 P_1 BK & \tau_M \overline{\varrho} \overline{\varepsilon}_1 P_1 BK \\ \tau_M \delta_1 \overline{\varepsilon}_1 P_1 BK & \tau_M \delta_1 \overline{\varepsilon}_1 P_1 BK \\ -\tau_M \delta_2 P_1 BK & -\tau_M \delta_2 P_1 BK \\ -\tau_M \delta_1 \delta_2 P_1 BK & -\tau_M \delta_1 \delta_2 P_1 BK \end{bmatrix}, \Xi_{52}^1 = \begin{bmatrix} \tau_M P_1 E & \tau_M \overline{\varepsilon} P_1 BK \\ 0 & \tau_M P_1 BK \\ 0 & 0 \\ 0 & 0 \end{bmatrix}$$

$$\Upsilon_{55}^1 = diag\{-P_1 S_1^{-1} P_1, -P_1 S_1^{-1} P_1, -P_1 S_1^{-1} P_1, -P_1 S_1^{-1} P_1\}$$

$$\Psi^2 = \begin{bmatrix} \Upsilon_{11}^2 & * & * & * & * \\ \Upsilon_{21}^2 & \Upsilon_{22}^2 & * & * & * \\ \Upsilon_{31}^2 & \Upsilon_{32}^2 & \Upsilon_{33}^2 & * & * \\ \Upsilon_{41}^2 & \Gamma_g^+ M_2 & 0 & -M_2 & * \\ \Upsilon_{51}^2 & 0 & 0 & \Upsilon_{54}^2 & \Upsilon_{55}^2 \end{bmatrix}$$

$$\Upsilon_{11}^2 = 2\rho_2 P_2 + P_2 A + A^T P_2 + H_2 - f_4 Z_2, \Upsilon_{21}^2 = f_4(Z_2^T - W_2^T), \Upsilon_{31}^2 = f_4 W_2$$
$$\Upsilon_{22}^2 = f_4(-2Z_2 + W_2 + W_2^T) - M_2 \Gamma_g^-, \Upsilon_{32}^2 = f_4(Z_2^T - W_2^T), \Upsilon_{33}^2 = -f_4 Z_2$$
$$\Upsilon_{41}^2 = E^T P_2, \Upsilon_{51}^2 = \eta_M P_2 A, \Upsilon_{54}^2 = \eta_M P_2 E, \Upsilon_{55}^2 = -P_2 S_2^{-1} P_2, f_4 = e^{-2\rho_2 \eta_M}$$

APPENDIX B. THE PROOF OF THEOREM 1

Proof. Choose the following Lyapunov functional candidate as

$$V_i(t) = V_{1i}(t) + V_{2i}(t) + V_{3i}(t) + V_{4i}(t) \tag{B1}$$

where

$$V_{1i}(t) = x^T(t) P_i x(t)$$
$$V_{2i}(t) = \int_{t-d_M}^t x^T(s)\mathcal{A}(\cdot) Q_i x(s) ds + \int_{t-\eta_M}^t x^T(s)\mathcal{A}(\cdot) H_i x(s) ds + \int_{t-\tau_M}^t x^T(s)\mathcal{A}(\cdot) J_i x(s) ds$$
$$V_{3i}(t) = d_M \int_{-d_M}^0 \int_{t+\theta}^t \dot{x}^T(s)\mathcal{A}(\cdot) R_i \dot{x}(s) ds d\theta + \eta_M \int_{-\eta_M}^0 \int_{t+\theta}^t \dot{x}^T(s)\mathcal{A}(\cdot) Z_i \dot{x}(s) ds d\theta$$
$$+ \tau_M \int_{-\tau_M}^0 \int_{t+\theta}^t \dot{x}^T(s)\mathcal{A}(\cdot) S_i \dot{x}(s) ds d\theta$$
$$V_{4i}(t) = \frac{1}{2}\pi^2(t) e^{2(-1)^i \rho_i t}$$

where $P_i > 0, Q_i > 0, H_i > 0, J_i > 0, R_i > 0, Z_i > 0, S_i > 0, \rho_i > 0 (i = 1, 2)$, $\theta < 0$ and $\mathcal{A}(\cdot) = e^{2(-1)^i \rho_i (t-s)}$.

By taking derivation and expectation on $V_i(x(t))$, one can get

$$\begin{aligned}
\mathbb{E}\{\dot{V}_{1i}(t)\} &= 2x^T(t)P_i\dot{x}(t)\\
\mathbb{E}\{\dot{V}_{2i}(t)\} &= x^T(t)(Q_i+H_i+J_i)x(t) - e^{-2\rho_i d_M}x^T(t-d_M)Q_ix(t-d_M)\\
&\quad - e^{-2\rho_i\eta_M}x^T(t-\eta_M)H_ix(t-\eta_M) - e^{-2\rho_i\tau_M}x^T(t-\tau_M)J_ix(t-\tau_M)\\
&\quad + 2(-1)^i\rho_i\int_{t-d_M}^{t} x^T(s)\mathcal{A}(\cdot)Q_ix(s)ds + 2(-1)^i\rho_i\int_{t-\eta_M}^{t} x^T(s)\mathcal{A}(\cdot)H_ix(s)ds\\
&\quad + 2(-1)^i\rho_i\int_{t-\tau_M}^{t} x^T(s)\mathcal{A}(\cdot)J_ix(s)ds\\
\mathbb{E}\{\dot{V}_{3i}(t)\} &= \dot{x}^T(t)(d_M^2R_i+\eta_M^2Z_i+\tau_M^2S_i)\dot{x}(t) - d_Me^{-2\rho_i d_M}\int_{t-d_M}^{t}\dot{x}^T(s)R_i\dot{x}(s)ds\\
&\quad - \eta_Me^{-2\rho_i\eta_M}\int_{t-\eta_M}^{t}\dot{x}^T(s)Z_i\dot{x}(s)ds - \tau_Me^{-2\rho_i\tau_M}\int_{t-\tau_M}^{t}\dot{x}^T(s)S_i\dot{x}(s)ds\\
&\quad + 2(-1)^i\rho_id_M\int_{-d_M}^{0}\int_{t+\theta}^{t}\dot{x}^T(s)\mathcal{A}(\cdot)R_i\dot{x}(s)dsd\theta + 2(-1)^i\rho_i\eta_M\int_{-\eta_M}^{0}\int_{t+\theta}^{t}\dot{x}^T(s)\mathcal{A}(\cdot)Z_i\dot{x}(s)dsd\theta\\
&\quad + 2(-1)^i\rho_i\tau_M\int_{-\tau_M}^{0}\int_{t+\theta}^{t}\dot{x}^T(s)\mathcal{A}(\cdot)S_i\dot{x}(s)dsd\theta\\
\mathbb{E}\{\dot{V}_{4i}(t)\} &= \left(\frac{1}{\pi(t)}-\sigma\right)e_k^T(t)\Omega e_k(t)e^{2(-1)^i\rho_i t} + (-1)^i\rho_i\pi^2(t)e^{2(-1)^i\rho_i t}
\end{aligned}$$

Inspired by the method in [38], we can get the following inequality:

$$\frac{1}{\pi(t)}e_k^T(t)\Omega e_k(t) - \sigma e_k^T(t)\Omega e_k(t) \le x^T(t-\tau(t))\Omega x(t-\tau(t)) - \sigma e_k^T(t)\Omega e_k(t) \tag{B2}$$

It is easy to acquire the following inequality with some simple calculation

$$\begin{aligned}
\mathbb{E}\{\dot{V}_i(t)\} &\le 2(-1)^i\rho_iV_i(t) + 2\rho_ix^T(t)P_ix(t) + (x^T(t-\tau(t))\Omega x(t-\tau(t)) - \sigma e_k^T(t)\Omega e_k(t))e^{2(-1)^i\rho_i t}\\
&\quad + 2x^T(t)P_i\dot{x}(t) + x^T(t)(Q_i+H_i+J_i)x(t) - e^{-2\rho_i d_M}x^T(t-d_M)Q_ix(t-d_M)\\
&\quad - e^{-2\rho_i\eta_M}x^T(t-\eta_M)H_ix(t-\eta_M) - e^{-2\rho_i\tau_M}x^T(t-\tau_M)J_ix(t-\tau_M)\\
&\quad + \dot{x}^T(t)(d_M^2R_i+\eta_M^2Z_i+\tau_M^2S_i)\dot{x}(t) - d_Me^{-2\rho_i d_M}\int_{t-d_M}^{t}\dot{x}^T(s)R_i\dot{x}(s)ds\\
&\quad - \eta_Me^{-2\rho_i\eta_M}\int_{t-\eta_M}^{t}\dot{x}^T(s)Z_i\dot{x}(s)ds - \tau_Me^{-2\rho_i\tau_M}\int_{t-\tau_M}^{t}\dot{x}^T(s)S_i\dot{x}(s)ds
\end{aligned}$$

By employing Lemma (1), it can be obtained

$$-d_Me^{-2\rho_i d_M}\int_{t-d_M}^{t}\dot{x}^T(s)R_i\dot{x}(s)ds \le e^{-2\rho_i d_M}\mu_1^T(t)\Xi_{1i}\mu_1(t) \tag{B3}$$

$$-\eta_Me^{-2\rho_i\eta_M}\int_{t-\eta_M}^{t}\dot{x}^T(s)Z_i\dot{x}(s)ds \le e^{-2\rho_i\eta_M}\mu_2^T(t)\Xi_{2i}\mu_2(t) \tag{B4}$$

$$-\tau_Me^{-2\rho_i\tau_M}\int_{t-\tau_M}^{t}\dot{x}^T(s)S_i\dot{x}(s)ds \le e^{-2\rho_i\tau_M}\mu_3^T(t)\Xi_{3i}\mu_3(t) \tag{B5}$$

where Ξ_{1i}, Ξ_{2i}, Ξ_{3i}, R_i, U_i, Z_i, W_i, S_i and $L_i(i=1,2)$ are matrices with appropriate dimensions, and

$$\Xi_{1i} = \begin{bmatrix} -R_i & * & * \\ R_i-U_i & -2R_i+U_i+U_i^T & * \\ U_i & R_i-U_i & -R_i \end{bmatrix},\ \Xi_{2i} = \begin{bmatrix} -Z_i & * & * \\ Z_i-W_i & -2Z_i+W_i+W_i^T & * \\ W_i & Z_i-W_i & -Z_i \end{bmatrix},$$

$$\Xi_{3i} = \begin{bmatrix} -S_i & * & * \\ S_i - L_i & -2S_i + L_i + L_i^T & * \\ L_i & S_i - L_i & -S_i \end{bmatrix}, \mu_1(t) = \begin{bmatrix} x(t) \\ x(t-d(t)) \\ x(t-d_M) \end{bmatrix}, \mu_2(t) = \begin{bmatrix} x(t) \\ x(t-\eta(t)) \\ x(t-\eta_M) \end{bmatrix},$$

$$\mu_3(t) = \begin{bmatrix} x(t) \\ x(t-\tau(t)) \\ x(t-\tau_M) \end{bmatrix}.$$

Based on the inequality (14) in Assumption 4, the following inequality can be acquired

$$x^T(x(t-d(t)))F^TFx(x(t-d(t))) - f^T(x(t-d(t)))f(x(t-d(t))) \geq 0 \tag{B6}$$

Since there exist matrices M_i and $N_i (i = 1, 2)$, by using Lemma 3, one can obtain

$$\begin{aligned} &\begin{bmatrix} x(t-\eta(t)) \\ g(x(t-\eta(t))) \end{bmatrix}^T \begin{bmatrix} -M_i\Gamma_g^- & M_i\Gamma_g^+ \\ \Gamma_g^+ M_i & -M_i \end{bmatrix} \begin{bmatrix} x(t-\eta(t)) \\ g(x(t-\eta(t))) \end{bmatrix} \geq 0 \\ &\begin{bmatrix} x(t-d(t)) \\ f(x(t-d(t))) \end{bmatrix}^T \begin{bmatrix} -N_i\Gamma_f^- & N_i\Gamma_f^+ \\ \Gamma_f^+ N_i & -N_i \end{bmatrix} \begin{bmatrix} x(t-d(t)) \\ f(x(t-d(t))) \end{bmatrix} \geq 0 \end{aligned} \tag{B7}$$

Next, two cases of $i = 1$ and $i = 2$ will be discussed, respectively.

When $i = 1$, one can obtain

$$\begin{aligned} \mathbb{E}\{\dot{x}^T(t)R_1\dot{x}(t)\} &= \mathcal{E}^TR_1\mathcal{E} + \delta_1^2\mathcal{F}^TR_1\mathcal{F} + \delta_2^2\mathcal{X}^TR_1\mathcal{X} + \delta_1^2\delta_2^2\mathcal{Y}^TR_1\mathcal{Y} \\ \mathbb{E}\{\dot{x}^T(t)Z_1\dot{x}(t)\} &= \mathcal{E}^TZ_1\mathcal{E} + \delta_1^2\mathcal{F}^TZ_1\mathcal{F} + \delta_2^2\mathcal{X}^TZ_1\mathcal{X} + \delta_1^2\delta_2^2\mathcal{Y}^TZ_1\mathcal{Y} \\ \mathbb{E}\{\dot{x}^T(t)S_1\dot{x}(t)\} &= \mathcal{E}^TS_1\mathcal{E} + \delta_1^2\mathcal{F}^TS_1\mathcal{F} + \delta_2^2\mathcal{X}^TS_1\mathcal{X} + \delta_1^2\delta_2^2\mathcal{Y}^TS_1\mathcal{Y} \end{aligned} \tag{B8}$$

where

$$\begin{aligned} \mathcal{E} &= BK(1-\overline{\varepsilon})(1-\overline{\varrho})[x(t-\tau(t)) + e_k(t)] + Eg(t-\eta(t)) + Ax(t) + BK\overline{\varepsilon}f(x(t-d(t))) \\ &\quad + BK(1-\overline{\varepsilon})\overline{\varrho}x_r(t) \\ \mathcal{F} &= BKf(x(t-d(t))) - \overline{\varrho}BKx_r(t) - (1-\overline{\varrho})BK(I+\Delta_r)[x(t-\tau(t)) + e_k(t)] \\ \mathcal{X} &= (1-\overline{\varepsilon})BKx_r(t) - (1-\overline{\varepsilon})BK(I+\Delta_r)[x(t-\tau(t)) + e_k(t)] \\ \mathcal{Y} &= -BKx_r(t) + BK(I+\Delta_r)[x(t-\tau(t)) + e_k(t)] \end{aligned}$$

Combining (B1)–(B8), one can derive the following inequality by using the Schur complement.

$$\begin{aligned} \mathbb{E}\{\dot{V}_1(t)\} \leq &-2\rho_1V_1(t) + \varpi_1^T(t)[\Upsilon_1 + d_M\mathbb{E}\{\dot{x}^T(t)R_1\dot{x}(t)\} + \eta_M\mathbb{E}\{\dot{x}^T(t)Z_1\dot{x}(t)\} \\ &+ \tau_M\mathbb{E}\{\dot{x}^T(t)S_1\dot{x}(t)\}]\varpi_1(t) \end{aligned}$$

where

$$\begin{aligned} \varpi_1(t) &= \begin{bmatrix} x^T(t) & \varphi_1(t) & \varphi_2(t) & \varphi_3(t) & \varphi_4(t) \end{bmatrix}^T, \varphi_1(t) = \begin{bmatrix} x^T(t-d(t)) & x^T(t-d_M) \end{bmatrix}, \\ \varphi_2(t) &= \begin{bmatrix} x^T(t-\eta(t)) & x^T(t-\eta_M) \end{bmatrix}, \varphi_3(t) = \begin{bmatrix} x^T(t-\tau(t)) & x^T(t-\tau_M) \end{bmatrix}, \\ \varphi_4(t) &= \begin{bmatrix} e_k^T(t) & x^T(t_r-\tau(t_r)) & e_k^T(t_r) & g^T(x(t-\eta(t))) & f^T(x(t-d(t))) \end{bmatrix} \end{aligned}$$

According to the inequality (28), one can get $\varpi_1^T(t)[\Upsilon_1 + d_M\mathbb{E}\{\dot{x}^T(t)R_1\dot{x}(t)\} + \eta_M\mathbb{E}\{\dot{x}^T(t)Z_1\dot{x}(t)\} + \tau_M\mathbb{E}\{\dot{x}^T(t)S_1\dot{x}(t)\}]\varpi_1(t) < 0$. Then, we can obtain $\mathbb{E}\{\dot{V}_1(t)\} \leq -2\rho_1V_1(t)$.

When $i = 2$, following the same analysis method, it is easy to get

$$\begin{aligned} \mathbb{E}\{\dot{V}_2(t)\} \leq &\, 2\rho_2V_2(t) + \varpi_2^T(t)[\Upsilon_2 + d_M\mathbb{E}\{\dot{x}^T(t)R_2\dot{x}(t)\} + \eta_M\mathbb{E}\{\dot{x}^T(t)Z_2\dot{x}(t)\} \\ &+ \tau_M\mathbb{E}\{\dot{x}^T(t)S_2\dot{x}(t)\}]\varpi_2(t) \end{aligned}$$

where $\varpi_2(t) = [x^T(t) \quad x^T(t-\eta(t)) \quad x^T(t-\eta_M) \quad g^T(x(t-\eta(t)))]^T$.

Based on the inequality (28), it can obtain $\varpi_2^T(t)[\Upsilon_2 + d_M\mathbb{E}\{\dot{x}^T(t)R_2\dot{x}(t)\} + \eta_M\mathbb{E}\{\dot{x}^T(t)Z_2\dot{x}(t)\} + \tau_M\mathbb{E}\{\dot{x}^T(t)S_2\dot{x}(t)\}]\varpi_2(t) < 0$, one can get $\mathbb{E}\{\dot{V}_2(t)\} \leq 2\rho_2 V_2(t)$.

Following the proposed method in Reference 37, for $t \in [t_{i,n}, t_{3-i,n+i-1})$, $i \in \{1,2\}$, $n \in \mathbb{N}$, it can be acquired

$$\mathbb{E}\{V_i(t)\} \leq e^{2(-1)^i\rho_i(t-t_{i,n})}\mathbb{E}\{V_i(t_{i,n})\}$$

where

$$t_{i,n} = \begin{cases} w_{n-1}, i = 1 \\ w_{n-1} + \epsilon_{n-1}, i = 2 \end{cases}$$

Then we have

$$\begin{cases} \mathbb{E}\{V_1(t)\} \leqslant e^{-2\rho_1(t-t_{1,n})}\mathbb{E}\{V_1(t)\}, & t \in [t_{1,n}, t_{2,n}) \\ \mathbb{E}\{V_2(t)\} \leqslant e^{2\rho_2(t-t_{2,n})}\mathbb{E}\{V_2(t)\}, & t \in [t_{2,n}, t_{1,n+1}) \end{cases} \tag{B9}$$

By combining the inequalities (29)–(31), it yields that

$$\begin{cases} \mathbb{E}\{V_1(t_{1,n})\} - a_2\mathbb{E}\{V_2(t_{1,n}^-)\} \leq 0 \\ \mathbb{E}\{V_2(t_{2,n})\} - a_1 e^{2(\rho_1+\rho_2)h}\mathbb{E}\{V_1(t_{2,n}^-)\} \leq 0 \end{cases} \tag{B10}$$

If $t \in [t_{1,n}, t_{2,n})$, the following inequality can be acquired by combining (B9) and (B10)

$$\begin{aligned} \mathbb{E}\{V_1(t)\} &\leq a_2 e^{-2\rho_1(t-t_{1,n})}\mathbb{E}\{V_2(t_{1,n}^-)\} \\ &\leq e^{\mathcal{F}(\cdot)\times 2(\rho_1+\rho_2)h + \mathcal{F}(\cdot)ln(a_1a_2)}\mathbb{E}\{V_1(0)\}e^d \\ &\leq e^{v_1(t)}\mathbb{E}\{V_1(0)\} \end{aligned}$$

where $d = 2\rho_2(w_n - w_{n-1} - \epsilon_{n-1} - \epsilon_{n-2} - \ldots - \epsilon_1 - \epsilon_0) - 2\rho_1(\epsilon_{n-1} + \epsilon_{n-2} + \ldots + \epsilon_1 + \epsilon_0)$, $v_1(t) = (\mathcal{T}_0 + \frac{t}{m_D}) \times 2(\rho_1 + \rho_2)h + 2\rho_2 c_{max}(\mathcal{T}_0 + \frac{t}{m_D}) - 2\rho_2\epsilon_{min}(\mathcal{T}_0 + \frac{t}{m_D}) + (\mathcal{T}_0 + \frac{t}{m_D})ln(a_1a_2)$.

Based on the equality (31), it can be obtained

$$\mathbb{E}\{V_1(t)\} \leq e^{p_1}e^{-st}\mathbb{E}\{V_1(0)\} \tag{B11}$$

where $p_1 = 2\mathcal{T}_0(\rho_1 + \rho_2)h + \mathcal{T}_0 ln(a_1a_2) + 2\rho_2 c_{max}\mathcal{T}_0 - 2\rho_1\epsilon_{min}\mathcal{T}_0$.

If $t \in [t_{2,n}, t_{1,n+1})$, it is easy to get

$$\mathbb{E}\{V_2(t)\} \leq \frac{\mathbb{E}\{V_1(0)\}}{a_2}e^{v_2(t)}$$

Then

$$\mathbb{E}\{V_2(t)\} \leq \frac{\mathbb{E}\{V_1(0)\}}{a_2}e^{p_2}e^{-st} \tag{B12}$$

where $v_2(t) = (\mathcal{T}_0 + \frac{t}{m_D} + 1) \times 2(\rho_1 + \rho_2)h + 2\rho_2 c_{max}(\mathcal{T}_0 + \frac{t}{m_D} + 1) - 2\rho_1\epsilon_{min}(\mathcal{T}_0 + \frac{t}{m_D} + 1) + (\mathcal{T}_0 + \frac{t}{m_D} + 1)ln(a_1a_2)$, $p_2 = (\mathcal{T}_0 + 1)(2(\rho_1 + \rho_2)h + ln(a_1a_2) + 2\rho_2 c_{max} - 2\rho_1\epsilon_{min})$.

Define $\mathcal{K} = max\{e^{p_1}, \frac{e^{p_2}}{a_2}\}$, $o_1 = min\{s_{min}(P_i)\}$, $o_2 = max\{s_{max}(P_i)\}$ and $o_3 = max\{s_{max}(P_i)\} + hs_{max}(Q_1) + \frac{h^2}{2}s_{max}(R_1 + Z_1)$.

By combining the equalities (B11) and (B12), it can be acquired

$$\mathbb{E}\{V_i(t)\} \leq \mathcal{K}e^{-st}\mathbb{E}\{V_1(0)\} \tag{B13}$$

Based on the definition of $V_i(t)$, it is easy to derive

$$\mathbb{E}\{V_i(t)\} \geq o_1\|x(t)\|^2, \mathbb{E}\{V_1(0)\} \leq o_3\|\varphi_0\|_h^2 \tag{B14}$$

Combining (B14) and (B13), one can get that

$$\mathbb{E}\{\|x(t)\|\} \leq \sqrt{\frac{\mathcal{K}o_3}{o_1}} e^{\alpha t}\|\varphi_0\|_h, \forall t \geq 0 \tag{B15}$$

That completes the proof. ∎

APPENDIX C. THE ELEMENTS OF THEOREM 2

$$\hat{\Psi}^1 = \begin{bmatrix} \hat{\Upsilon}_{11}^1 & * & * & * & * \\ \hat{\Upsilon}_{21}^1 & \hat{\Upsilon}_{22}^1 & * & * & * \\ \hat{\Upsilon}_{31}^1 & \hat{\Upsilon}_{32}^1 & \hat{\Upsilon}_{33}^1 & * & * \\ \hat{\Upsilon}_{41}^1 & \hat{\Upsilon}_{42}^1 & 0 & \hat{\Upsilon}_{44}^1 & * \\ \hat{\Upsilon}_{51}^1 & \hat{\Upsilon}_{52}^1 & 0 & 0 & \hat{\Upsilon}_{55}^1 \end{bmatrix}$$

$$\hat{\Upsilon}_{11}^1 = \begin{bmatrix} \hat{\Theta}_{11}^1 & * & * & * & * & * & * & * \\ \hat{\Theta}_{21}^1 & \hat{\Theta}_{22}^1 & * & * & * & * & * & * \\ \hat{\Theta}_{31}^1 & \hat{\Theta}_{32}^1 & \hat{\Theta}_{33}^1 & * & * & * & * & * \\ \hat{\Theta}_{41}^1 & 0 & 0 & \hat{\Theta}_{44}^1 & * & * & * & * \\ \hat{\Theta}_{51}^1 & 0 & 0 & \hat{\Theta}_{54}^1 & \hat{\Theta}_{55}^1 & * & * & * \\ \hat{\Theta}_{61}^1 & 0 & 0 & 0 & 0 & \hat{\Theta}_{66}^1 & * & * \\ \hat{\Theta}_{71}^1 & 0 & 0 & 0 & 0 & \hat{\Theta}_{76}^1 & \hat{\Theta}_{77}^1 & * \\ \hat{\Theta}_{81}^1 & 0 & 0 & 0 & 0 & 0 & 0 & -\hat{\Omega} \end{bmatrix}$$

$$\hat{\Theta}_{11}^1 = 2\rho_1 X_1 + X_1 A + A^T X_1 + \hat{Q}_1 + \hat{H}_1 + \hat{J}_1 - f_1\hat{R}_1 - f_2\hat{Z}_1 - f_3\hat{S}_1, f_1 = e^{-2\rho_1 d_M}$$

$$\hat{\Theta}_{21}^1 = f_1(\hat{R}_1^T - \hat{U}_1^T), \hat{\Theta}_{22}^1 = f_1(-2\hat{R}_1 + \hat{U}_1^T + \hat{U}_1) - \hat{N}_1\Gamma_f^- + X_1 F^T F X_1$$

$$\hat{\Theta}_{31}^1 = f_1\hat{U}_1^T, f_2 = e^{-2\rho_1\eta_M}, \hat{\Theta}_{32}^1 = f_1(\hat{R}_1^T - \hat{U}_1^T), \hat{\Theta}_{33}^1 = f_1(\hat{Q}_1 - \hat{R}_1), f_3 = e^{-2\rho_1\tau_M}$$

$$\hat{\Theta}_{41}^1 = f_2(\hat{Z}_1^T - \hat{W}_1^T), \hat{\Theta}_{51}^1 = f_2\hat{W}_1, \hat{\Theta}_{44}^1 = f_2(-2\hat{Z}_1 + \hat{W}_1 + \hat{W}_1^T) - \hat{M}_1\Gamma_g^-$$

$$\hat{\Theta}_{54}^1 = f_2(\hat{Z}_1^T - \hat{W}_1^T), \hat{\Theta}_{55}^1 = f_2(\hat{H}_1 - \hat{Z}_1), \hat{\Theta}_{61}^1 = (I + \Delta_r)\overline{\varrho}_1\overline{\varepsilon}_1 Y^T B^T + f_3\hat{S}_1 - f_3\hat{L}_1$$

$$\Theta_{66}^1 = f_3(-2\hat{S}_1 + \hat{L}_1 + \hat{L}_1^T), \hat{\Theta}_{71}^1 = f_3\hat{L}_1^T, \hat{\Theta}_{76}^1 = f_3(\hat{S}_1^T - \hat{L}_1^T), \hat{\Theta}_{77}^1 = f_3(J_1 - \hat{S}_1)$$

$$\hat{\Theta}_{81}^1 = (I + \Delta_r)\overline{\varrho}_1\overline{\varepsilon}_1 Y^T B^T, \overline{\varepsilon}_1 = 1 - \overline{\varepsilon}, \overline{\varrho}_1 = 1 - \overline{\varrho}, \delta_1 = \sqrt{\overline{\varepsilon}\,\overline{\varepsilon}_1}, \delta_2 = \sqrt{\overline{\varrho}\,\overline{\varrho}_1}$$

$$\hat{\Upsilon}_{21}^1 = \begin{bmatrix} \overline{\varrho}\overline{\varepsilon}_1 Y^T B^T & 0 & 0 & 0 & 0_{1\times4} \\ \overline{\varrho}\overline{\varepsilon}_1 Y^T B^T & 0 & 0 & 0 & 0_{1\times4} \\ X_1 E^T & 0 & 0 & \Gamma_g^+\hat{M}_1 & 0_{1\times4} \\ \overline{\varepsilon} Y^T B^T & \Gamma_f^+\hat{N}_1 & 0 & 0 & 0_{1\times4} \end{bmatrix}$$

$$\Upsilon_{22}^1 = \{\sigma\hat{\Omega}, -\hat{\Omega}, -\hat{M}_1, -\hat{N}_1\}, \hat{\Upsilon}_{31}^1 = \begin{bmatrix} \hat{\Lambda}_{31}^1 & \hat{\Xi}_{31}^1 \end{bmatrix}, \hat{\Upsilon}_{32}^1 = \begin{bmatrix} \hat{\Lambda}_{32}^1 & \hat{\Xi}_{32}^1 \end{bmatrix}$$

$$\hat{\Lambda}_{31}^1 = \begin{bmatrix} d_M A X_1 & 0_{1\times4} & d_M\overline{\varrho}_1\overline{\varepsilon}_1 BY \\ 0 & 0_{1\times4} & d_M(I + \Delta_r)\delta_1\overline{\varepsilon}_1 BY \\ 0 & 0_{1\times4} & d_M(I + \Delta_r)\delta_2 BY \\ 0 & 0_{1\times4} & -d_M\delta_1\delta_2 BY \end{bmatrix}, \hat{\Xi}_{31}^1 = \begin{bmatrix} 0 & d_M\overline{\varrho}_1\overline{\varepsilon}_1 BY \\ 0 & d_M(I + \Delta_r)\delta_1\overline{\varepsilon}_1 BY \\ 0 & d_M(I + \Delta_r)\delta_2 BY \\ 0 & -d_M\delta_1\delta_2 BY \end{bmatrix}$$

$$\hat{\Xi}_{32}^{1}=\begin{bmatrix} d_M EX_1 & d_M\bar{\varepsilon}BY \\ 0 & d_M BY \\ 0 & 0 \\ 0 & 0 \end{bmatrix}, \hat{\Lambda}_{32}^{1}=\begin{bmatrix} d_M\bar{\varrho}\bar{\varepsilon}_1 BY & d_M\bar{\varrho}\bar{\varepsilon}_1 BY \\ d_M\delta_1\bar{\varepsilon}_1 BY & d_M\delta_1\bar{\varepsilon}_1 BY \\ -d_M\delta_2 BY & -d_M\delta_2 BY \\ -d_M\delta_1\delta_2 BY & -d_M\delta_1\delta_2 BY \end{bmatrix}$$

$$\hat{\Upsilon}_{33}^{1}=diag\{-2e_{11}X_1+e_{11}^2\hat{R}_1, -2e_{11}X_1+e_{11}^2\hat{R}_1-2e_{11}X_1+e_{11}^2\hat{R}_1, -2e_{11}X_1+e_{11}^2\hat{R}_1\}$$

$$\hat{\Lambda}_{41}^{1}=\begin{bmatrix} \eta_M AX_1 & 0_{1\times 4} & \eta_M\bar{\varrho}_1\bar{\varepsilon}_1 BY \\ 0 & 0_{1\times 4} & \eta_M(I+\Delta_r)\delta_1\bar{\varepsilon}_1 BY \\ 0 & 0_{1\times 4} & \eta_M(I+\Delta_r)\delta_2 BY \\ 0 & 0_{1\times 4} & -\eta_M\delta_1\delta_2 BY \end{bmatrix}, \hat{\Xi}_{41}^{1}=\begin{bmatrix} 0 & \eta_M\bar{\varrho}_1\bar{\varepsilon}_1 BY \\ 0 & \eta_M(I+\Delta_r)\delta_1\bar{\varepsilon}_1 BY \\ 0 & \eta_M(I+\Delta_r)\delta_2 BY \\ 0 & -\eta_M\delta_1\delta_2 BY \end{bmatrix}$$

$$\hat{\Upsilon}_{41}^{1}=\begin{bmatrix} \hat{\Lambda}_{41}^{1} & \hat{\Xi}_{41}^{1} \end{bmatrix}, \hat{\Upsilon}_{42}^{1}=\begin{bmatrix} \hat{\Lambda}_{42}^{1} & \hat{\Xi}_{42}^{1} \end{bmatrix}, \hat{\Upsilon}_{51}=\begin{bmatrix} \hat{\Lambda}_{51}^{1} & \hat{\Xi}_{51}^{1} \end{bmatrix}, \hat{\Upsilon}_{52}=\begin{bmatrix} \hat{\Lambda}_{52}^{1} & \hat{\Xi}_{52}^{1} \end{bmatrix}$$

$$\hat{\Lambda}_{42}^{1}=\begin{bmatrix} \eta_M\bar{\varrho}\bar{\varepsilon}_1 BY & \eta_M\bar{\varrho}\bar{\varepsilon}_1 BY \\ \eta_M\delta_1\bar{\varepsilon}_1 BY & \eta_M\delta_1\bar{\varepsilon}_1 BY \\ -\eta_M\delta_2 BY & -\eta_M\delta_2 BY \\ -\eta_M\delta_1\delta_2 BY & -\eta_M\delta_1\delta_2 BY \end{bmatrix}, \hat{\Xi}_{42}^{1}=\begin{bmatrix} \eta_M EX_1 & \eta_M\bar{\varepsilon}BY \\ 0 & \eta_M BY \\ 0 & 0 \\ 0 & 0 \end{bmatrix}$$

$$\hat{\Upsilon}_{44}^{1}=diag\{-2e_{12}X_1+e_{12}^2\hat{Z}_1, -2e_{12}X_1+e_{12}^2\hat{Z}_1-2e_{12}X_1+e_{12}^2\hat{Z}_1, -2e_{12}X_1+e_{12}^2\hat{Z}_1\}$$

$$\hat{\Lambda}_{51}^{1}=\begin{bmatrix} \tau_M AX_1 & 0_{1\times 4} & \tau_M\bar{\varrho}_1\bar{\varepsilon}_1 BY \\ 0 & 0_{1\times 4} & \tau_M(I+\Delta_r)\delta_1\bar{\varepsilon}_1 BY \\ 0 & 0_{1\times 4} & \tau_M(I+\Delta_r)\delta_2 BY \\ 0 & 0_{1\times 4} & -\tau_M\delta_1\delta_2 BY \end{bmatrix}, \hat{\Xi}_{51}^{1}=\begin{bmatrix} 0 & \tau_M\bar{\varrho}_1\bar{\varepsilon}_1 BY \\ 0 & \tau_M(I+\Delta_r)\delta_1\bar{\varepsilon}_1 BY \\ 0 & \tau_M(I+\Delta_r)\delta_2 BY \\ 0 & -\tau_M\delta_1\delta_2 BY \end{bmatrix}$$

$$\hat{\Lambda}_{52}^{1}=\begin{bmatrix} \tau_M\bar{\varrho}\bar{\varepsilon}_1 BY & \tau_M\bar{\varrho}\bar{\varepsilon}_1 BY \\ \tau_M\delta_1\bar{\varepsilon}_1 BY & \tau_M\delta_1\bar{\varepsilon}_1 BY \\ -\tau_M\delta_2 BY & -\tau_M\delta_2 BY \\ -\tau_M\delta_1\delta_2 BY & -\tau_M\delta_1\delta_2 BY \end{bmatrix}, \hat{\Xi}_{52}^{1}=\begin{bmatrix} \tau_M EX_1 & \tau_M\bar{\varepsilon}BY \\ 0 & \tau_M BY \\ 0 & 0 \\ 0 & 0 \end{bmatrix}$$

$$\hat{\Upsilon}_{55}^{1}=diag\{-2e_{13}X_1+e_{13}^2\hat{S}_1, -2e_{13}X_1+e_{13}^2\hat{S}_1-2e_{13}X_1+e_{13}^2\hat{S}_1, -2e_{13}X_1+e_{13}^2\hat{S}_1\}$$

$$\hat{\Psi}^{2}=\begin{bmatrix} \hat{\Upsilon}_{11}^{2} & * & * & * & * \\ \hat{\Upsilon}_{21}^{2} & \hat{\Upsilon}_{22}^{2} & * & * & * \\ \hat{\Upsilon}_{31}^{2} & \hat{\Upsilon}_{32}^{2} & \hat{\Upsilon}_{33}^{2} & * & * \\ \hat{\Upsilon}_{41}^{2} & \Gamma_g^{+}M_2 & 0 & -\hat{M}_2 & * \\ \hat{\Upsilon}_{51}^{2} & 0 & 0 & 0 & \hat{\Upsilon}_{55}^{2} \end{bmatrix}$$

$$\hat{\Upsilon}_{11}^{2}=2\rho_2X_2+X_2A+A^TX_2H_2-f_4\hat{Z}_2+F^TF, \hat{\Upsilon}_{21}^{2}=f_4(\hat{Z}_2^T-\hat{W}_2^T), \hat{\Upsilon}_{31}^{2}=f_4\hat{W}_2$$

$$\hat{\Upsilon}_{22}^{2}=f_4(-2\hat{Z}_2+\hat{W}_2+\hat{W}_2^T)-M_2\Gamma_g^{-}, \hat{\Upsilon}_{32}^{2}=f_4(\hat{Z}_2^T-\hat{W}_2^T), \hat{\Upsilon}_{33}^{2}=-f_4\hat{Z}_2$$

$$\hat{\Upsilon}_{41}^{2}=X_2E^T, \hat{\Upsilon}_{51}^{2}=\eta_M AX_2, \hat{\Upsilon}_{54}^{2}=\eta_M EX_2, \hat{\Upsilon}_{55}^{2}=-2e_{13}X_2+e_{13}^2\hat{S}_2, f_4=e^{-2\rho_2\eta_M}$$

APPENDIX D. THE PROOF OF THEOREM 2

Proof. When $i=1$, the matrix Ψ^1 can be equivalently expressed as follows

$$\Psi^1=\tilde{\Psi}^1+sym\{H_e^T\Delta_r H_f\} \tag{D1}$$

where

$$\tilde{\Psi}^1 = \begin{bmatrix} \tilde{\Upsilon}^1_{11} & * & * & * & * \\ \Upsilon^1_{21} & \Upsilon^1_{22} & * & * & * \\ \tilde{\Upsilon}^1_{31} & \Upsilon^1_{32} & \Upsilon^1_{33} & * & * \\ \tilde{\Upsilon}^1_{41} & \Upsilon^1_{42} & 0 & \Upsilon^1_{44} & * \\ \tilde{\Upsilon}^1_{51} & \Upsilon^1_{52} & 0 & 0 & \Upsilon^1_{55} \end{bmatrix}$$

$$\tilde{\Upsilon}^1_{11} = \begin{bmatrix} \Theta^1_{11} & * & * & * & * & * & * & * \\ \Theta^1_{21} & \Theta^1_{22} & * & * & * & * & * & * \\ \Theta^1_{31} & \Theta^1_{32} & \Theta^1_{33} & * & * & * & * & * \\ \Theta^1_{41} & 0 & 0 & \Theta^1_{44} & * & * & * & * \\ \Theta^1_{51} & 0 & 0 & \Theta^1_{54} & \Theta^1_{55} & * & * & * \\ \Theta^1_{61} & 0 & 0 & 0 & 0 & \Theta^1_{66} & * & * \\ \Theta^1_{71} & 0 & 0 & 0 & 0 & \Theta^1_{76} & \Theta^1_{77} & * \\ \Theta^1_{81} & 0 & 0 & 0 & 0 & 0 & 0 & -\Omega \end{bmatrix}$$

$$\tilde{\Upsilon}^1_{31} = \begin{bmatrix} \tilde{\Lambda}^1_{31} & \tilde{\Xi}^1_{31} \end{bmatrix}, \tilde{\Upsilon}^1_{41} = \begin{bmatrix} \tilde{\Lambda}^1_{41} & \tilde{\Xi}^1_{41} \end{bmatrix}, \tilde{\Upsilon}^1_{51} = \begin{bmatrix} \tilde{\Lambda}^1_{51} & \tilde{\Xi}^1_{51} \end{bmatrix},$$

$$\tilde{\Lambda}^1_{31} = \begin{bmatrix} d_M P_1 A & 0_{1\times4} & d_M \bar{\varrho}_1 \bar{\varepsilon}_1 P_1 BK \\ 0 & 0_{1\times4} & d_M \delta_1 \bar{\varepsilon}_1 P_1 BK \\ 0 & 0_{1\times4} & d_M \delta_2 P_1 BK \\ 0 & 0_{1\times4} & -d_M \delta_1 \delta_2 P_1 BK \end{bmatrix}, \tilde{\Xi}^1_{31} = \begin{bmatrix} 0 & d_M \bar{\varrho}_1 \bar{\varepsilon}_1 P_1 BK \\ 0 & d_M \delta_1 \bar{\varepsilon}_1 P_1 BK \\ 0 & d_M \delta_2 P_1 BK \\ 0 & -d_M \delta_1 \delta_2 P_1 BK \end{bmatrix}$$

$$\tilde{\Theta}^1_{61} = \bar{\varrho}_1 \bar{\varepsilon}_1 K^T B^T P_1 + f_3 \tau_M S_1 - f_3 \tau_M L_1, \tilde{\Theta}^1_{81} = \bar{\varrho}_1 \bar{\varepsilon}_1 K^T B^T P_1$$

$$\tilde{\Lambda}^1_{41} = \begin{bmatrix} \eta_M P_1 A & 0_{1\times4} & \eta_M \bar{\varrho}_1 \bar{\varepsilon}_1 P_1 BK \\ 0 & 0_{1\times4} & \eta_M \delta_1 \bar{\varepsilon}_1 P_1 BK \\ 0 & 0_{1\times4} & \eta_M \delta_2 P_1 BK \\ 0 & 0_{1\times4} & -\eta_M \delta_1 \delta_2 P_1 BK \end{bmatrix}, \tilde{\Xi}^1_{41} = \begin{bmatrix} 0 & \eta_M \bar{\varrho}_1 \bar{\varepsilon}_1 P_1 BK \\ 0 & \eta_M \delta_1 \bar{\varepsilon}_1 P_1 BK \\ 0 & \eta_M \delta_2 P_1 BK \\ 0 & -\eta_M \delta_1 \delta_2 P_1 BK \end{bmatrix}$$

$$\tilde{\Lambda}^1_{51} = \begin{bmatrix} \tau_M P_1 A & 0_{1\times4} & \tau_M \bar{\varrho}_1 \bar{\varepsilon}_1 P_1 BK \\ 0 & 0_{1\times4} & \tau_M \delta_1 \bar{\varepsilon}_1 P_1 BK \\ 0 & 0_{1\times4} & \tau_M \delta_2 P_1 BK \\ 0 & 0_{1\times4} & -\tau_M \delta_1 \delta_2 P_1 BK \end{bmatrix}, \tilde{\Xi}^1_{51} = \begin{bmatrix} 0 & \tau_M \bar{\varrho}_1 \bar{\varepsilon}_1 P_1 BK \\ 0 & \tau_M \delta_1 \bar{\varepsilon}_1 P_1 BK \\ 0 & \tau_M \delta_2 P_1 BK \\ 0 & -\tau_M \delta_1 \delta_2 P_1 BK \end{bmatrix}$$

$$H_e = \begin{bmatrix} H_{e1} & H_{e2} & H_{e3} \end{bmatrix}, H_f = \begin{bmatrix} 0_{1\times5} & K & 0 & K & 0_{1\times16} \end{bmatrix}$$

$$H_{e1} = \begin{bmatrix} \bar{\varrho}_1 \bar{\varepsilon}_1 P_1 B & 0_{1\times12} & d_M \delta_1 \bar{\varepsilon}_1 P_1 B & d_M \delta_2 P_1 B & 0 \end{bmatrix}$$

$$H_{e2} = \begin{bmatrix} 0 & \eta_M \delta_1 \bar{\varepsilon}_1 P_1 B & \eta_M \delta_2 P_1 B & 0 \end{bmatrix}$$

$$H_{e3} = \begin{bmatrix} 0 & \tau_M \delta_1 \bar{\varepsilon}_1 P_1 B & \tau_M \delta_2 P_1 B & 0 \end{bmatrix}$$

By utilizing the Lemma 2, the following inequality can be obtained

$$\tilde{\Psi}^1 + m_1 \kappa^2 H_e^T \Delta_r^2 H_e + m_1^{-1} H_f^T H_f < 0 \tag{D2}$$

Then, according to $\Delta_r^2 < \kappa^2$, one can get

$$\tilde{\Psi}^1 + m_1 H_e^T H_e + m_1^{-1} H_f^T H_f < 0 \tag{D3}$$

By using Schur complement, the equality (D3) can be rewritten as follows

$$\Pi^1 = \begin{bmatrix} \tilde{\Psi}^1 & * & * \\ \kappa H_e & -m_1 I & * \\ H_f & 0 & -m_1^{-1} I \end{bmatrix} \tag{D4}$$

For given positive scalars e_{11}, e_{12}, e_{13}, due to

$$\begin{cases} (R_1 - e_{11}P_1)R_1^{-1}(R_1 - e_{11}P_1) \geq 0 \\ (Z_1 - e_{12}P_1)Z_1^{-1}(Z_1 - e_{12}P_1) \geq 0 \\ (S_1 - e_{13}P_1)S_1^{-1}(S_1 - e_{13}P_1) \geq 0 \end{cases} \tag{D5}$$

From (D5), one can get

$$\begin{cases} -P_1R_1^{-1}P_1 \leq -2e_{11}P_1 + e_{11}^2 R_1 \\ -P_1Z_1^{-1}P_1 \leq -2e_{12}P_1 + e_{12}^2 Z_1 \\ -P_1S_1^{-1}P_1 \leq -2e_{13}P_1 + e_{13}^2 S_1 \end{cases} \tag{D6}$$

By replacing $-P_1R_1^{-1}P_1$, $-P_1Z_1^{-1}P_1$, $-P_1S_1^{-1}P_1$ in Υ_{33}^1, Υ_{44}^1, Υ_{55}^1 with $-2e_{11}P_1 + e_{11}^2 R_1$, $-2e_{12}P_1 + e_{12}^2 Z_1$, $-2e_{13}P_1 + e_{13}^2 S_1$, respectively.

When $i = 1$, define $X_1 = P_1^{-1}$, $\varsigma_1 = diag\{\underbrace{X_1, \ldots, X_1}_{24}, I, I\}$, $Y = KX_1$, $\hat{Q}_1 = X_1Q_1X_1^T$, $\hat{R}_1 = X_1R_1X_1^T$, $\hat{U}_1 = X_1U_1X_1^T$, $\hat{W}_1 = X_1W_1X_1^T$, $\hat{L}_1 = X_1L_1X_1^T$, $\hat{S}_1 = X_1S_1X_1^T$, $\hat{Z}_1 = X_1Z_1X_1^T$, $\hat{H}_1 = X_1H_1X_1^T$, $\hat{J}_1 = X_1J_1X_1^T$, $\hat{M}_1 = X_1M_1X_1^T$, $\hat{N}_1 = X_1N_1X_1^T$. Pre- and post- multiplying both sides of Π^1 with ς_1 and its transpose, one can get $\hat{\Psi}^1$. When $i = 2$, following the method above, the matrix $\hat{\Psi}^2$ also can be acquired. In addition, pre- and post- multiplying the inequalities in (29) with X_2 and X_1, respectively, then by utilizing the Schur complement, we can obtain that (33)–(34) imply (29). Similarly, one can conclude that the inequalities in (35)–(37) imply (30). Thus, the system (26) is exponentially mean-square stable. According to $Y = KX_1$, it is easy to get $K = YX_1^{-1}$.

This completes the proof. ■